Isotopic Composition of Terrestrial Rare Gases and Application to Earth Science

by

Keisuke Nagao
Okayama University of Science

1979

Abstract.

Isotopic and elemental compositions of rare gases were investigated in gas samples collected in the Japanese Islands. He in volcanic gas, hot-spring gas, geothermal well gas samples, and most of bubble gas samples in low temperature water pool showed significantly high $^{3}He/^{4}He$ ratios, about 7 times the atmospheric ratio of 1.4×10^{-6}, in spite of the large variation of He concentration, and showed no systematic differences in the $^{3}He/^{4}He$ ratios among the gas sources. Emanations of mantle He enriched in primordial He proved common phenomena in the Japanese Islands. The origin of mantle He will be discussed.

Soil gas samples collected in the Nigorikawa geothermal area showed evidence for mass fractionation of the atmospheric rare gases. This means that several per cent enrichment of ^{20}Ne relative to ^{22}Ne is not a sufficient condition for identifying a primordial component of Ne in the earth.

An enrichment of ^{20}Ne relative to ^{22}Ne was found in volcanic gases. The enrichment could not be explained as the mass fractionation of the atmospheric Ne. The origin of the enrichment will be discussed.

$^{40}Ar/^{36}Ar$ ratios in gas samples investigated were lower than 325. The contribution of radiogenic ^{40}Ar was relatively small in all samples.

Elemental abundance patterns of rare gases were similar to that of the atmospheric rare gases dissolved in low temperature water, or were enriched in Kr and Xe relative to the later pattern. The enrichment in Kr and Xe will be discussed.

$^{3}He/^{4}He$ and $^{4}He/^{20}Ne$ ratios in volcanic gases from Mt. Showa-shinzan decreased and approached to the atmospheric values with time. This suggests the declination of volcanic activity. High $^{3}He/^{4}He$ ratio, about 6.5 times the atmospheric ratio, first observed in gas samples collected at the earthquake fault zone in Matsushiro earthquake swarm strongly suggests that the $^{3}He/^{4}He$ ratio is possible measure for the detection of earthquake precursors. High $^{3}He/^{4}He$ ratios found in hot-spring gases show that the addition of magmatic volatiles to the ground water is one of the heat sources of hot-springs.

Continental CO_2 well gases, Mid-Atlantic Ridge basalts, and volcanic lava were also analyzed for rare gas isotopic compositions. $^{3}He/^{4}He$ ratios of Ridge basalts were about 1.0×10^{-5}, whereas the ratios of continental CO_2 well gases were about 5×10^{-7}. Enrichment of light isotope of Ar in volcanic lava could be understood in terms of the mass fractionation of the atmospheric Ar.

Contents.

I Introduction.

Studies on the elemental abundances and the isotopic compositions of rare gases in terrestrial and extraterrestrial materials give useful information on the origin and evolution of the solar system, and have shown that there exist five components of rare gases of different origins: 1) a radiogenic component, 2) a fissiogenic component, 3) a cosmogenic component, 4) a trapped component of primordial, ambient gases in the early solar nebula absorbed by meteorite matters, 5) an atmospheric component. These components were acquired by the materials through physical processes such as the decay of natural radioactivity, the production by particle bombardment, and trapping of ambient gases. The quantitative determination of these components enables us to calculate gas-retention ages and cosmic-ray exposure ages of meteorites and lunar samples, to estimate the concentration of extinct nuclides such as ^{129}I and ^{244}Pu and thereby to calculate the formation interval between the end of nucleosynthesis and the beginning of gas retention in the meteoritic materials. The primordial, trapped component gives information regarding the circumstances in the primitive solar nebula at the formation of solar system.

In addition to the information from meteorites and lunar samples, the recent artificial space-crafts give valuable information on the rare gas compositions in the atmosphere of other planets such as Venus and Mars. The comparative investigation of rare gas compositions among the planets is important for the study of the origin and evolution of the planets and the solar system. Our knowledge on the rare gas compositions in the solid earth, however, was quite poor relative to high quality data on those in extraterrestrial materials

such as meteorites and lunar samples. Since the terrestrial rare gases are used as a reference rare gas composition in the investigation of the origin and evolution of planets and the solar system, high quality data of rare gases on the terrestrial materials are required.

Terrestrial rare gases give also useful information on the origin and evolution of the earth's atmosphere. Brown[1] showed that the rare gases in the earth's atmosphere are highly depleted relative to the solar abundances and concluded that the earth's atmosphere was not a trapped primitive solar nebula but degassed from the interior of the earth. Two types of degassing models have been proposed for the formation of earth's atmosphere: continuous and catastrophic degassing models. Rubey[2] showed that the estimated excess volatiles in the earth's atmosphere and ocean could be accounted by volatiles degassed via volcanic gases and hot-spring emanation, and proposed a continuous degassing model for the formation of the atmosphere. Though a continuous degassing model[e.g. 3,4] and a catastrophic one[e.g. 5,6] have been proposed, it is still controversial which model is valid for the formation of the atmosphere. Ozima and Kudo[4] first discussed the degassing history based on the $^{40}Ar/^{36}Ar$ ratio. The $^{40}Ar/^{36}Ar$ ratio for primordial Ar has been calculated to be 10^{-4} based on a nucleo-synthetic theory[7]. The ratio is increasing with time because of the production of radiogenic ^{40}Ar by the decay of ^{40}K. Hence the concentration of ^{40}Ar and $^{40}Ar/^{36}Ar$ ratio in the earth's interior depends on the concentration of K and the degassing rate. Assuming a value of about 2,000 for the $^{40}Ar/^{36}Ar$ ratio in the present mantle, Ozima[8] proposed a catastrophic degassing model in the early stage of the

earth evolution. The determination of $^{40}Ar/^{36}Ar$ ratio as well as the concentration of Ar in the present mantle is important for the study of degassing history of the earth.

Recent observations of juvenile rare gas emanations should also provide a constraint on the earth-atmosphere evolution models. Excess ^{129}Xe was detected in CO_2 well gas from New Mexico[9 ,10], in lava rock from New Mexico[11] and in xenolithic rocks from Hawaii[12, 14, 31]. Excess ^{129}Xe in these samples has been regarded to be evidence for the presence of extinct $^{129}I(t_{1/2} = 1.7 \times 10^7 yr)$ at the period of degassing of the earth, and to support a catastrophic degassing model in the early stage of the earth.

Early works on the isotopic composition of terrestrial He were carried out for continental natural gases and minerals containing radioactive elements. Observed $^3He/^4He$ ratios were lower than the atmospheric ratio of 1.4×10^{-6}, because of the enrichment in radiogenic ^4He from U and Th[15]. However, recent isotopic analyses of He in volcanic gases[16-19], in oceanic water[20-24], oceanic basalts[25-27] and in mantle-derived minerals[28-32] have shown high $^3He/^4He$ ratios. The highest $^3He/^4He$ ratio reported attains to 4.9×10^{-5}[32], 35 times the atmospheric ratio. The high $^3He/^4He$ ratio has been interpreted as evidence that primordial He which has found in meteorites and lunar samples[33-35] is still emanating from the mantle[17]. If this is the case, the identification of primordial components as well as the determination of $^{40}Ar/^{36}Ar$ ratio in the mantle are important in studying the degassing history of the earth and the origin of the earth itself.

The identification of primordial rare gas component also gives useful information about the earth sciences. As will be given

later, the high $^3He/^4He$ ratio was first observed in gas samples collected at an earthquake fault zone in the Matsushiro earthquake swarm[36], which suggests that the observation of $^3He/^4He$ ratio may be useful for the detection of earthquake precursors. Such high ratios were also detected in all the hot-spring gases analyzed. This suggests the emanation of volatiles as a heat transport from a magma.

High $^3He/^4He$ ratios relative to the atmospheric value have been detected mainly in pillow basalts collected at oceanic ridges where the new crust is formed from the mantle, in rocks and minerals solidified in the mantle and in samples from hot-spots. Hence, the high $^3He/^4He$ ratio is regarded to represent the ratio in the upper mantle underlying oceanic ridges and hot-spots. In contrast to these area, the Japanese Island Arc is located on a subducting zone of the oceanic plate. We are interested in identifying the component of He with high $^3He/^4He$ ratio in samples collected in the sbduction zone. Craig et al.[18] detected a high $^3He/^4He$ ratio, about 6 times the atmospheric ratio, in a fumarolic gas from a Hakone fumarole. Wakita et al.[36] also detected a similar value of the $^3He/^4He$ ratio in gas samples collected at the earthquake fault region in the Matsushiro earthquake swarm. These results suggested that He with the high $^3He/^4He$ ratio is also being released in the Japanese Islands as well as in the oceanic ridges and the hot-spots. We have investigated the isotopic compositions of rare gases in volcanic gases, hot-spring gases, bubble gases in low temperature water pool, geothermal well gases in the Japanese Islands.

In this thesis we describe results on the isotopic compositions of He and other rare gases and the primordial component of He in gas samples of various sources and discuss an application to the earth

sciences such as a detection of earthquake precursors and a heat source of hot-springs.

II . Experimental techniques.

1) Sampling localities and chemical compositions.

Sampling localities in the Japanese Islands and classification of samples are given in Fig. II -1. The sample number and the classification used in Fig. II -1 are summarized in Table II -1 with the localities and the date of collection. CO_2 well gases sampled in Derbecen, Hungary and Mid-Atlantic Ocean ridge basalts are not included in Fig. II -1. In Table II -1, samples are labeled according to the classification as follows; free-gas in hot-spring(H-), volcanic gas(V-), bubble gas in low temperature water pool(L-), soil gas(S-), geothermal prospecting well gas(G-), well gas for earthquake prediction (W-), CO_2-well gas in Derbecen, Hungary(DR-), Atlantic ridge basalt (RB-) and volcanic lava in Japan(VL-). Chemical compositions of gas samples in literature are summarized in Table II -2.

2) Collection of gas samples.

a) Bubble gas in water pool.

Collection vessels were made of borosilicate glass, the inside volume of which was about 100 cm^3. Another type of collection vessels were made of Pyrex glass and the inside volume was about 20 cm^3. Vaccum tight stop-cocks were attached to both sides of the vessels. At the sampling field, a funnel and a manual pump were attached to each side of the collection vessel with a thick wall plastic tube and the funnel was dipped in water pool as shown in Fig. II -2a. First, the plastic tube and the sampling vessel were filled with local water through the funnel with the aid of the manual pump, and then the funnel was placed on the bubbling site to collect the gas.

The water was replaced by the gas in the funnel with great care to avoid the atmospheric contamination. Then the gas in the funnel was transfered into the sampling vessel by replacing the water. In order to minimize the atmospheric contamination, the vessel was flushed several times by the sample gas collected in the funnel.

b) Collection of soil gas.

Soil gas samples were collected by a usual procedure for the CO_2 prospecting method. A pipe of 1 m in length and 1.5 cm in diameter was sealed in a hole of 1 m in depth and 5 cm in diameter with bentonite as shown in Fig.II-2b. The pipe was riddled at the lower end and the upper end was capped with a Tygon tube closed by a pinch-cock. It was left sealed for a day and the gas accumulated in the hole was introduced into a 20 cm^3 volume of Pyrex-glass sampling vessel as shown in Fig. II-2b. The vessel was flushed several times with the sample gas to remove the atmospheric contamination and then the stop-cocks were closed.

c) Collection of fumarolic gas.

The fumarolic gases subjected to rare gas analyses in this work were collected by Matsuo, Mizutani and Matsubayashi. The sampling technique of fumarolic gas has been shown elsewhere[37, 38]. The fumarolic gas was introduced into alkaline solution to remove the acid component and the water-vapor. The non-absorbed component of gas was stored in borosilicate-glass# or Pyrex-glass vessel by sealing off the ends with a torch.

SB-glass by Shibata glass factory.

3) Mass spectrometry.

a) Splitting of gas samples.

For the rare gas analyses, the collected gas samples were split into several ampoules of various volumes with breacable seals. The pressure and the temperature of gas sample at splitting were measured and used for calculation of rare gas concentrations. After the rare gas analyses, the inside volume of ampoule was also determined. The concentration of rare gas was calculated by,

$$C = \frac{v\ P_0\ T}{V\ P\ T_0} \times 10^6 \qquad (\text{in ppm}) \qquad \text{(Eq. II-1)}$$

where v = total amount of rare gas isotope in the ampoule determined mass spectrometrically

V = inside volume of the ampoule

P = pressure of the gas sample at splitting

T = temperature of the gas sample at splitting

P_0 = 760 Torr

T_0 = 273 K

b) Apparatus for rare gas analysis.

The mass spectrometer and the low blank metal system for rare gas analysis used in this work have been described elsewhere[39]. The line for rare gas analysis, schematically represented in Fig. II-3, was consisted of a rare gas extraction and purification system, a calibration sample preparation system and a mass spectrometer. The mass spectrometer was of a single focussing 90° sector type with 20 cm of ion curvature and equipped with a ten-stage Cu-Be secondary electron multiplier. The resolving power was adjusted to about 600 to separate ^3He from H_3 and HD peaks. A trace of He spectrum is shown in Fig. II-4. Hydrocarbon peaks were also

separated from isobaric Ar, Kr and Xe isotopes. To reduce the interference of ^{20}Ne and ^{22}Ne with doubly-charged ^{40}Ar and CO_2 ions, respectively, an electron accelaration voltage in the ion source was set at 40V.

c) Mass analysis.

The sample gas was introduced into the purification system by breaking the breakable seal and purified with Ti-Zr getters heated at 750°C. He and Ne were separated by adsorbing Ar, Kr and Xe on activated charcoal at liquid nitrogen temperature, and were admitted to the mass spectrometer for isotopic analysis. Ar, Kr and Xe were then separated each other by selective desorption on charcoal trap at -50°C, -30°C and 100°C. Temperature of the charcoal trap was controled by N_2 gas vaporized from liquid nitrogen. The vaporization rate was controled by monitoring temperature at the charcoal trap with a thermo-couple. Inside the charcoal trap CH2, fins were attached to improve the heat conductivity. The improved adsorbing power for Ar at liquid nitrogen temperature enabled us to analyze Ne with minimum interference with Ar^{++} ions in the mass spectrometer. A small volume of about 8 cm^3 designated as V_r in Fig. II-3 was used to reduce the quantity of gas to a suitable amount for mass spectrometry.

Rare gases introduced into the mass spectrometer were analyzed for the isotopic compositions. Known amounts of the atmospheric rare gases were also analyzed with the same procedure as applied for the sample gases to determine the sensitivity of the mass spectrometer and to correct the mass discrimination. The mass discrimination in He was determined by analyzing an artificial mixture of pure ^3He and ^4He, the $^3He/^4He$ ratio of which was 1.34×10^{-4}.

The doubly-charged ^{40}Ar and CO_2 ions interfering with ^{20}Ne and ^{22}Ne, respectively, were corrected with the measured $^{40}Ar^{++}/^{40}Ar^{+}$ and CO_2^{++}/CO_2^{+} ratios. Correction for CO_2^{++} at ^{22}Ne was less than 1 per cent and $^{40}Ar^{++}$ correction was also negligible for gas samples collected in the Japanese Island. However, CO_2^{++} correction attained to several per cent of ^{22}Ne for samples DR05, DR63 and DR65 because of very low abundance of Ne.

The $^{21}Ne/^{20}Ne$ ratio was affected by an accidental appearence of $^{20}NeH^{+}$ ions. The appearence of ^{20}NeH varied depending on pressure of He and Ne in the ion source. Fig. II-5 shows the variation of $(^{21}Ne + ^{20}NeH)/^{20}Ne$ ratio against the total amount of He and Ne admitted in the mass spectrometer. However, as shown in Fig. II-5, the $^{22}Ne/^{20}Ne$ ratio is approximately constant at a wide range of the ion source pressure. The appearence of $^{20}NeH^{+}$ ions relative to ^{20}Ne varied from 7.5×10^{-4} for 1×10^{-8} cm^3STP of He and Ne to 7×10^{-5} for 1×10^{-5} cm^3STP of He and Ne. We could not clarify how the hydride ions appeared. Because the occurrence of ^{20}NeH ions was affected by an adjustment of electric field in the ion source, the appearence of ^{20}NeH could be attributed to a drawing out efficiency of ^{20}NeH varied by a change in electric field caused by different intensity of ion beam in the ion source, or by a difference between the sites where the ^{20}NeH and rare gas ions were produced. Hence, the hydride ions may not appere in a condition of different adjustment of ion source in the mass spectrometer or in other mass spectrometers.

The $^{21}Ne/^{20}Ne$ ratio was corrected based on the correl
in Fig. II-5. However, uncertainty was relatively large. Therefore the $^{21}Ne/^{20}Ne$ ratio was less reliable than the $^{22}Ne/^{20}Ne$ ratio.

The sensitivities of the mass spectrometer for He and Ne were also affected by the elevated pressure of He and Ne in the mass spectrometer as shown in Fig. II-6. Where 5×10^{-5} cm^3STP of a He and Ne mixture was admitted to the mass spectrometer, the sensitivities decreased by about factor of 2 and 3 for He and Ne, respectively, relative to those with 10^{-8} cm^3STP of the gases. Hence, the concentrations of He and Ne were determined with the amounts of He and Ne in the spectrometer lower than 1×10^{-7} cm^3 STP, where the variations of sensitivities were within 10 per cent.

Ⅲ. Results.

1) Isotopic compositions and elemental abundances of rare gases.

Isotopic compositions are compiled in Table Ⅲ-1. Sample numbers used in Table Ⅲ-1 are summarized in Table Ⅱ-1. The rare gas concentrations were calculated by Eq. Ⅱ-1. In this calculation, no correction was applied for the removed acid-forming gases in most of the volcanic gases. The correction for the removed components can be estimated with the chemical composition of gas samples listed in Table Ⅱ-2.

2) $^3He/^4He$ ratios and He concentrations.

a) Distribution of $^3He/^4He$ ratios in the Japanese Islands.

The $^3He/^4He$ ratios relative to the atmospheric $^3He/^4He$ ratio defined by,

$$R = \frac{(^3He/^4He)_{sample}}{(^3He/^4He)_{atmosphere}} \qquad \text{(Eq. Ⅲ-1)}$$

are shown in Fig. Ⅲ-1, where the atmospheric $^3He/^4He$ ratio is 1.4×10^{-6}. The symboles which represent the classification of gas samples used in Fig. Ⅲ-1 are same as used in Fig. Ⅱ-1. Samples except well gases Wl-MT and Wl-KW were all enriched in ^3He relative to the atmospheric ratio. The highest value of R = 11 was found in Gl-ON, a geothermal prospecting well gas at Onuma, Akita prefecture. ^3He enrichments, about seven times the atmospheric value, were found in many other samples. This shows that the emanations of He enriched in ^3He are common phenomena in the Japanese Islands.

b) correlation between $^3He/^4He$ and $^4He/^{20}Ne$ ratios.

The $^3He/^4He$ ratios for all gas samples and Mid-Atlantic Ridge basalts are plotted against the $^4He/^{20}Ne$ ratios in Fig. III-2. A mixing line represents a composition of a mixture between the atmosphere and a He-enriched gas with a high $^3He/^4He$ ratio of 1.0×10^{-5}. All data lie on or below the mixing line, except for sample Gl-ON whose $^3He/^4He$ ratio is significantly higher than the others. The $^3He/^4He$ ratios below the mixing line can be interpreted as admixture of radiogenic ^4He accumulated in crustal rock. Fig. III-2 also shows that there is no systematic difference in the $^3He/^4He$ ratios among volcanic, hot-spring and low temperature bubble gases. An upper limit of $^3He/^4He$ ratios for these gases is approximately 1.0×10^{-5}.

To estimate the mixing ratio of He from various origins, three components were assumed as follows.

	atmospheric He	crustal He	mantle He
$^3He/^4He$	1.4×10^{-6}	3×10^{-8}	1.0×10^{-5}
$^4He/^{20}Ne$	0.32	∞	$> 10^4$

A high $^4He/^{20}Ne$ ratio assumed for the mantle component is supported by the result for oceanic ridge basalt RB197 whose $^4He/^{20}Ne$ and $^3He/^4He$ ratios were 1900 and 1.0×10^{-5}, respectively. Higher $^4He/^{20}Ne$ ratios have been reported for natural diamonds by Takaoka and Ozima[28, 29] and for Mid-Atlantic Ridge basalts by Craig and Lupton[27]. The $^3He/^4He$ ratios higher than 6 times the atmospheric ratio support that the rare gases in diamonds and ridge basalts are of mantle origin. The $^3He/^4He$ and $^4He/^{20}Ne$ ratios observed in this work can be expressed as,

$$\left[\frac{^3He}{^4He}\right]_{ob.} = (1.4a + 0.03c + 10m) \times 10^{-6} \qquad (\text{Eq. III-2a})$$

$$\left[\frac{^4He}{^{20}Ne}\right]_{ob.} = \frac{0.32}{a} \qquad (\text{Eq. III-2b})$$

$$a + c + m = 1 \qquad (\text{Eq. III-2c})$$

where "a", "c" and "m" represent the mixing ratio of ^4He for atmospheric, crustal and mantle He, respectively. In Eq. III-2b, ^{20}Ne of mantle-origin was neglected.

Correlation between the calculated $^3He/^4He$ and $^4He/^{20}Ne$ ratios are shown in Fig. III-3. Atmospheric contamination in ^4He is less than 10 per cent if the $^4He/^{20}Ne$ ratio is more than ten times the atmospheric ratio. Fig. III-2 and Fig. III-3 indicate that most of samples with high $^4He/^{20}Ne$ ratios contain He composed mainly of mantle He with a high $^3He/^4He$ ratio and of a minor component of crustal He enriched in radiogenic ^4He.

In contrast, samples W1-MT, W2-KW, DR05, DR63 and DR65 show low $^3He/^4He$ ratios of 10^{-7}, which is a typical $^3He/^4He$ ratio for crustal He. Two samples W1-MT and W2-KW were collected in wells used for the detection of earthquake precursors in the Keihin district. This area is covered with thick "Kanto Loam", the volcanic ashes ejected from Hakone and Fuji volcanoes, and there is no volcanic activity. Other three samples, DR05, DR63 and DR65 were collected in CO_2 wells at Derbecen in Hungary, the depths of which were 865m, 1170m and 1060m, respectively. The area is characterized by thick sedimentary materials and by a high heat flow[40].

c) $^3He/^4He$ ratios and He concentrations.

The $^3He/^4He$ ratios for gas samples are plotted against the He

concentrations in Fig. III-4. Acid components in most of the volcanic gas samples were removed with alkaline solution. For such samples, the He concentrations should be lower than those plotted in Fig. III-4. In spite of the wide variation of He concentration from 0.6 to 1800 ppm, no significant correlation was found between the $^3He/^4He$ ratio and the He concentration. High $^3He/^4He$ ratios relative to the atmospheric one were found in samples with various He concentrations. High concentrations of more than 1000 ppm He were found in hot-spring gases H2-SR, H9-KI and H10-MT. He concentrations for most of the samples range from several to several ten ppm. Hungary CO_2 gases DR05, DR63 and DR65 were highly enriched in radiogenic ^4He.

d) Correlation between He concentration and chemical composition.

The concentrations of He in natural gases and liquid samples have been measured to survey the He resources in Japan since 1922 [41-45]. Recently, systematic surveys were carried out by the Geological Survey of Japan[46-56]. These surveys showed that the Japanese natural gases could be grouped into three types according as their chemical composition; CO_2-, N_2- and CH_4-types of gases. The He concentration was highest in the N_2-type gas, whereas in the CO_2-type gas the He concentration was very low.

The He concentrations determined in this work are plotted against the CO_2 and N_2 concentrations in Fig. III-5. Samples H6-YM, H7-MS and S2-MN with He concentrations higher than several hundred ppm are enriched in N_2. In contrast, samples H1-IW, L5-IS and L3-YS show high CO_2 and low He concentrations. This correlation between the He concentration and the chemical composition is consistent with the previous observation noted above.

Such correlation was not applicable to the continental CO_2 well

gases DR05, DR63 and DR65 because of the high concentration of radiogenic ^4He.

e) Correlation between $^3He/^4He$ ratios and CO_2 concentrations in gas samples from the Nigorikawa geothermal area.

The Nigorikawa geothermal area is located in a caldera about 20 km north-west of Mt. Komagatake, one of the largest active volcanoes in Hokkaido. The locality is shown in Fig. II-1. The area is known to have showings of oil, natural gas, hot-spring as well as gaseous geothermal surface manifestations. The last eruptive activity has been dated to be 12,900 $\pm$ 270 y.B.P. by means of a ^{14}C dating method[57].

Samples consisted of bubble gas (designated as L1-NG) collected at an abundand sulfer mine and five soil gases S1-NG-1 ~ S1-NG-5 collected within 500 m of the bubble site. *In-situ* analysis of the CO_2 concentration in the soil gas was carried out with a portable interferometer analyser. High $^3He/^4He$ ratios relative to the atmospheric He were found in all samples. The $^3He/^4He$ ratios correlate with the CO_2 concentration as well as the He/Ne ratios. Fig. III-6 shows the correlation between $^3He/^4He$ ratios and CO_2 concentrations for six samples. Sample L1-NG with the $^3He/^4He$ ratio of seven times the atmospheric ratio consists of 96.8% CO_2, 1.6% N_2, 0.9% H_2S, 0.7% CH_4 and trace of H_2[58]. Fig. III-6 shows that a high $^3He/^4He$ ratio accompanies a high CO_2 concentration and the soil gas samples lie around the line connecting the points represent samples L1-NG and the atmosphere.

Analyses of CO_2 concentrations in soil gases are used for the determination of suitable point for the geothermal development. The correlation shown in Fig. III-6 suggests that the analysis of

$^{3}He/^{4}He$ ratio in soil gas is also applicable to this purpose.

3) Isotopic compositions of Ne and Ar.

As noted in Section II-3, hydride ions have prevented precise determination of the $^{21}Ne/^{20}Ne$ ratio. Hence, only the $^{22}Ne/^{20}Ne$ ratio will be discussed.

Fig. III-7 shows a correlation diagram of $\delta(22/20)$ and $\delta(38/36)$. A mass fractionation line of atmospheric Ne and Ar is defined by

$$\delta(m/m_0;\ atm) = K(X)[(m-m_0)/\{(m+m_0)/2\}] \qquad (\text{Eq. III-3})$$

$\delta(m/m_0;\ atm)$ is defined by

$$\delta(m/m_0;\ atm) = [(^{m}X/^{m_0}X)/(^{m}X/^{m_0}X)_{atm} - 1] \times 10^{3} \qquad (\text{Eq. III-4})$$

where ^{m}X and ^{m_0}X represent a rare gas element X of mass m and m_0, and subscript "atm" means atmospheric. K(X) in Eq. III-3 is the mass fractionation per fractional mass difference.

Most of the samples lie around the atmospheric value, for which the mass fractionation effect is within 10 per mil for both $\delta(22/20)$ and $\delta(38/36)$. However, large deviation from the atmospheric value is found in the soil gas of Nigorikawa and the volcanic gases.

As will be discussed later, the samples of Nigorikawa lie on the mass fractionation line through the atmospheric value, $\delta(22/20) = \delta(38/36) = 0$. In contrast to the Nigorikawa gases, the volcanic gas samples, V1-TK, V2-SS-4, V2-SS-6, V3-US, V4-NS, V7-KJ and V9-SI-1 show large isotopic deviations from the atmospheric value and define another mass fractionation line parallel to the mass fractionation line defined by Nigorikawa soil gas samples. In Fig. III-7, the

$\delta(22/20)$ values for volcanic gases range from -53 per mil to about - 10 per mil along the new mass fractionation line, the intercept of which at $\delta(38/36) = 0$ is about -20 per mil, corresponding to $^{22}Ne/^{20}Ne = 0.100$. This isotopic composition of Ne will be discussed in Section Ⅳ-3.

All the data of Ar except for the CO_2 gases from Hungary and for the oceanic ridge basalts are plotted in Fig. Ⅲ-8, where $\delta(38/36)$ and $\delta(40/36)$ represent the deviation of Ar isotopic ratios from the atmospheric composition as defined by Eq. Ⅲ-4. The mass fractionation line through the atmospheric value is defined by Eq. Ⅲ-3. Fig. Ⅲ-8 indicates that the isotopic composition of Ar can be understood as a mixture of mass fractionated Ar and radiogenic ^{40}Ar.

$^{40}Ar/^{36}Ar$ ratios observed in most of Japanese gas samples show small enrichment in radiogenic ^{40}Ar relative to the atmospheric $^{40}Ar/^{36}Ar$ ratio of 295.5. The highest $^{40}Ar/^{36}Ar$ ratio investigated was 325. Such high $^{40}Ar/^{36}Ar$ ratios have been reported in volcanic gases of Kamchatka[16] which is located near the subduction zone and is tectonically similar to the Japanese Islands.

The Nigorikawa soil gases, volcanic lava and some of gas samples lie on the mass fractionation line and show low $^{38}Ar/^{36}Ar$ and $^{40}Ar/^{36}Ar$ ratios relative to the atmospheric values.

4) Isotopic compositions of Kr and Xe.

Isotopic compositions of Kr and Xe were atmospheric within experimental errors except for the Nigorikawa soil gases S1-NG-1 and S1-NG-4 which showed systematic enrichment in light isotopes. Fig. Ⅲ-9a and Fig. Ⅲ-9b show the isotopic compositions of Kr and Xe in samples S1-NG-1 and S1-NG-4 with delta values defined by

Eq. III-4. Such light isotope enrichments are seen in the Ne and Ar isotopic compositions and in the elemental abundances of rare gases in these samples. The Nigorikawa gas samples will be discussed in Section IV-2.

5) Elemental abundance patterns of rare gases in gas samples.

Elemental abundances relative to the atmospheric rare gases are shown in Fig. III-10. F(m) is defined by

$$F(m) = ({}^{m}X/{}^{36}Ar)/({}^{m}X/{}^{36}Ar)_{atm} \qquad (\text{Eq. III-5})$$

where ${}^{m}X$ and subscript "atm" represent a rare gas element X of mass m and atmospheric, respectively. A fractionated abundance pattern which represents the atmospheric rare gases dissolved in low temperature water[59] is also plotted in Fig. III-10 for comparison.

The elemental abundance patterns of Ne, Ar, Kr and Xe showed no appreciable difference among the gas samples of various sources. These abundance patterns are similar to a type 1 pattern classified by Ozima and Alexander[60], which was interpreted as the fractionation of the atmospheric rare gases established by the low temperature solubility into water.

Significant enrichments in He were found in all of the samples analyzed for the elemental abundances. As discussed in Section IV-1, most of He in these samples are mantle-derived He enriched in ${}^{3}He$. Enrichment of He should be attributed to relatively large mobility of He in the interior of the earth.

Ⅳ. Discussion.

1) Origin of high $^3He/^4He$ ratio in terrestrial materiales.

Early works on the isotopic composition of terrestrial He were carried out for the continental natural gases and minerals containing radioactive elements[15]. Observed $^3He/^4He$ ratios were lower than the atmospheric ratio of 1.4×10^{-6} because of radiogenic ^4He from U and Th. However, recent analyses of the $^3He/^4He$ ratio in volcanic gases[16-19], oceanic water[20-24], oceanic basalts[25-27], and mantle-derived minerals[28-32] have shown high $^3He/^4He$ ratios attaining to 4.9×10^{-5}[32], 35 times the atmospheric ratio.

Several hypotheses have been proposed to explain the high $^3He/^4He$ ratios by Mamyrin et al.[17]. They were: 1) mass fractionation of atmospheric He caused by migration, 2) decay of technogenic tritium ($t_{1/2}$ = 12.26yr) dissolved in meteoric water, 3) nuclear processes to produce ^3He in the interior of the earth, 4) emanation of primordial He, the $^3He/^4He$ ratio of which is similar to He found in meteorites and solar wind.

It is difficult to estimate the enrichment in ^3He caused by mass fractionation because of the only two stable isotopes of He. Nagao et al.[61] indicated evidence for the mass fractionation of rare gases in soil gas samples. For the most fractionated sample, ^3He enrichment caused by the mass fractionation was estimated to be several ten per cent relative to the atmospheric ratio. This enrichment cannot explain the observed high $^3He/^4He$ ratios.

High concentration of technogenic tritium such as several hundreds tritium units (= 10^{-18}atomsT/atomH) observed in meteoric water in 1963 and 1964 could produce high $^3He/^4He$ ratio if the meteoric water remained in underground with no mixing of water of different origin

and no addition of atmospheric or radiogenic He. However, such condition in nature is difficult for all the volcanic and hot-spring gas samples with high $^3He/^4He$ ratios. Craig et al.[18] estimated that the maximum contribution of technogenic tritium in fumarolic gas from Hakone was 1 per cent of the observed ^3He concentration. Moreover, the technogenic tritium can not explain the high $^3He/^4He$ ratios found in oceanic ridge basalts and mantle-derived minerals which have solidified before the appearence of technogenic tritium.

Mamyrin et al.[17] listed the considerable nuclear reactions to produce tritium or ^3He and pointed out the most probable reaction was $^6Li(n,\alpha)T$ because of the large cross-section of 950 barns for thermal neutrons. Neutrons are produced from fission and (α, n) reactions in the interior of the earth. However, the theoretical production ratio of ^3He relative to ^4He is 10^{-7} for granitic rock and 10^{-8} 10^{-9} for radioactive minerals[62]. These ratios are lower than the atmospheric ratio of 1.4×10^{-6}.

A remaining possible source of He with a high $^3He/^4He$ ratio is the primordial component of He, the $^3He/^4He$ ratio of which is of the order of 10^{-4} found in meteorites and lunar samples[33-35]. The high $^3He/^4He$ ratios found in the terrestrial samples can be understood in terms of mixing between the primordial He and radiogenic He enriched in ^4He.

Mamyrin et al.[17] concluded that the primordial component was the most probable source of the high $^3He/^4He$ ratio. This means that the primordial component of He is now emanated from the deep interior of the earth.

2) He in the Japanese Islands.

High $^3He/^4He$ ratios relative to the atmospheric value were observed in most of gas samples collected in the Japanese Islands.

Craig et al.[18] pointed out that the $^3He/^4He$ ratios in volcanic gases of circum-Pacific continental-margine are about 7 times the atmospheric ratio, ranging from 8×10^{-6} to 1.1×10^{-5}. Volcanic gases in the Kamchatka Peninsula, tectonically similar to the Japanese Island Arc, also showed similar $^3He/^4He$ ratios. The highest ratio reported was 8.1 times the atmospheric value[16].

The $^3He/^4He$ ratios with high $^4He/^{20}Ne$ ratios (Fig. Ⅲ-2) determined in this work are consistent with those value reported by Craig et al.[18] and Kamenskiy[16] for volcanic gases of circum-Pacific continental margine. These ratios are somewhat lower than the ratio observed in glassy margine of ridge basalts, volcanic gas of Hawaii and mantle-derived minerals such as diamonds, the ratios of which presumably represent the $^3He/^4He$ ratio in the mantle.

Where is the He found in the Japanese Islands released from? A model of a tectonic structure under the Japanese Islands is illustrated in Fig. Ⅳ-1. If the $^3He/^4He$ ratio in the subducting oceanic plate of Pacific Ocean is considered, radiogenic ^4He produced by *in situ* decay of U and Th is admixed to initial He which represents the $^3He/^4He$ ratio of upper mantle. The contribution of accumulated radiogenic ^4He to the initial He is approximately calculated by,

$$\frac{R}{R_0} = \frac{1}{0.173\ t \times \frac{[U]}{[He]} + 1} \qquad \text{(Eq. Ⅳ-1)}$$

where R_0 and R are the $^3He/^4He$ ratios for initial and present-day He, respectively, and t is the age of the plate in my. [U] and [He] are U concentration in ppm and the initial He concentration in 10^{-6} cm^3STP/g, respectively. The U/Th ratio is assumed to be 1.8[63]. Loss of He from the plate and the contamination of atmospheric He

dissolved in the penetrating oceanic water were neglected. If for the downgoing plate under the Japanese Islands, t = 100my, [U] = 0.1 ppm and [He] = 10 x 10^{-6} cm^3STP/g are assumed, the $^3He/^4He$ ratio at present will be $0.85R_0$. If $^3He/^4He = 1.4 \times 10^{-5}$, which is the ratio observed in fresh glassy margine of oceanic basalts[27], is assumed for R_0, the $^3He/^4He = 1.2 \times 10^{-5}$, 8.6 times the atmospheric, is calculated for He in the present downgoing plate. Hence, we can understand the observed $^3He/^4He$ ratio in gas samples in this work by this model. The U concentration in oceanic ridge basalts reported by Aument and Hyndman[64] ranged from 0.19 to 0.70 ppm, whereas some of the glassy margins of oceanic basalts showed the U concentration less than 0.1 ppm[65]. The He concentration in ridge basalts reported by Lupton and Craig[26] and Craig and Lupton[27] are lower than that used above, 10 x 10^{-6} cm^3STP/g. For Pacific ridge basalts He concentrations are less than 2 x 10^{-6} cm^3STP/g[27]. Mid Atlantic ridge basalts RB-56 and RB-197 in Table III-1 also show about 3 x 10^{-6} cm^3STP/g.

If for the U concentration in Pacific oceanic plate, more than 0.2 ppm is adopted, R will be less than $0.37R_0$, which correspond to the $^3He/^4He$ ratio less than 5.2×10^{-6} for $R_0 = 1.4 \times 10^{-5}$. In Cretaceous deep-sea basalt near the southern end of the Bermuda Rise, which has been estimated to be 108 my old[66], the $^3He/^4He$ ratio of $(3 \pm 1) \times 10^{-6}$ has been observed by Takaoka and Nagao[67]. Such a value of $^3He/^4He$ ratio seems to support the estimation. If this is the case, He released from the remelting subduction plate under the Japanese Islands can not explain the observed high $^3He/^4He$ ratio in gas samples.

However, the observed U and He concentrations are from only the upper surface of the oceanic plate which is several ten km thick.

U concentration in the upper mantle was estimated to be less than 0.05 ppm[68-70] from geochemical and geothermal studies. If 0.05 ppm is adopted for an upper limit of U concentration and initial He concentration of 2×10^{-6} cm^3STP/g is assumed, R is higher than $0.7R_0$ which corresponds to $^3He/^4He = 9.8 \times 10^{-6}$ for $R_0 = 1.4 \times 10^{-5}$. Hence, to resolve this question, the concentrations of U and He in deeper part of the oceanic plate must be determined.

Another possible source is the deeper part of the mantle from which He up-rises through the melted layer[71] along the upper surface of subducting plate. There the uniform $^3He/^4He$ ratio of about 1.0×10^{-5} will be produced by mixing of ^3He-enriched mantle He and radiogenic ^4He in the surface of the plate.

Other source seems to be related to the mechanism of production of magma. If the magma is produced by partial melt of mantle above the downgoing plate caused by the up-rising water released from the plate, He in the plate will be admixed to the He in the partially melted mantle. Such a process suggests the same isotopic composition of He in fresh basalts and andesites as in gas samples. The $^3He/^4He$ ratio in fresh igneous rocks should be determined.

A high $^3He/^4He$ ratio of $(1.54 \pm 0.04) \times 10^{-5}$, 11 times the atmospheric value, was found in Onuma geothermal well gas Gl-ON. The ratio is identical to that found in oceanic ridge basalts[26, 27]. Since this sample is the only one sample analyzed for the $^3He/^4He$ ratio in north-east of Japan. An extensive survey is required in this district to understand the high $^3He/^4He$ ratio observed in Onuma gas sample.

As can be seen in Fig. III-1, all samples with high $^3He/^4He$ ratios were collected inside the volcanic front and the two samples

with low $^3He/^4He$ ratio of about 10^{-7} were collected outside it. To know whether the regional difference in the $^3He/^4He$ ratio exist, isotopic analyses of He in samples outside the volcanic front are required.

Untill the high $^3He/^4He$ ratio is ubiquitousely found in the natural gases occurring in the Japanese Islands, He in gas and liquid samples observed in the previous He surveys[40-56] mentioned in Section Ⅲ-2d was suposed to be radiogenic He produced by α-decays of U and Th in crustal rocks, especially in granitic rocks underlying the area. He with a high $^3He/^4He$ ratio should be attributed to He in a deep interior of the earth such as the mantle.

Fig. Ⅲ-5 indicates that the He concentration is higher in N_2-rich gases than in CO_2-rich gases, while the $^3He/^4He$ ratios in both gas samples are practically same. This indicates that the N_2 gas with high He content is not an atmospheric contamination. A source of the N_2 gas seems to be an oceanic sedimentary materials on the descending plate. Matsuo et al.[37] also attributed the N_2 gas in volcanic gases to recycled N_2 gas released by the decomposition of organic materials on the descending oceanic plate based on the high N_2/Ar ratios observed in both the volcanic gases and the organic materials in oceanic sediments.

The low He concentration in CO_2-rich gas can be understood as dilution of mantle-derived He with the CO_2 gas produced by chemical reactions in crustal materials. It has been proposed by Wakita et al.[36] that the CO_2-rich gas, L2-MC, with 5ppm He collected at the Matsushiro earthquake fault zone can be explained as the production of CO_2 by the chemical reaction of hydrochloric acid from a magma with calcareous matter.

He is escaping from the upper atmosphere to the inter-planetary space and He in the atmosphere is considered to be in a steady state now. Hence, estimation of He flux from the solid earth into the atmosphere is important for the He budget in the atmosphere. Early works on ^3He[e.g.73] did not consider the flux of primordial ^3He from the earth's interior.

After the detection of primordial He, Craig et al.[72] estimated the oceanic flux of ^3He to be 4 ± 1 atoms cm^{-2} sec^{-1}, and pointed out that the primordial ^3He emanation was sufficient to account for the calculated escape rate of ^3He by Johnson and Axford[73].

Estimation of ^3He flux in the Japanese Islands is difficult because of the lack of data for the flux of volcanic, hot-spring and other types of gases. Our estimation of ^3He emanation for hot-springs Shiramine and Koyahara are 2×10^{12} and 4×10^{11} atoms sec^{-1}, respectively. Averaged flux of ^3He estimated in Shimane and Yamagata prefectures based on the $^3He/^4He$ ratios obtained in this work and the flux and the He concentrations of hot-spring gases reported by Hirukawa et al.[55] and Maki et al.[48] are 0.2 and 0.6 atom ^3He cm^{-2} sec^{-1}, respectively. Since the density of hot-springs is high in the area, the averaged ^3He flux from hot-springs in the Japanese Islands should be lower than those values.

Because the data on the out flow of fumarolic gases and erupted volcanic gases in the Japanese Islands was not available, the estimation of ^3He flux in these gases was difficult. Released energy from a small eruption of volcano is comparable with the energy released from a superior hot-spring in a year. If it is assumed that the ^3He flux is proportional to the released energy from hot-spring and volcanic activity, ^3He flux in volcanic gases is not significant because of the lower density of volcanoes relative to that of hot-springs and because of the long interval between the eruptions.

From these estimation the ^{3}He flux averaged in the Japanese Islands may not exceed 1 atom $^{3}He\ cm^{-2}\ sec^{-1}$. Further investigation of ^{3}He flux requires the determination of volatile flux from the hot-springs, volcanoes and other types of gas emanations.

3) Isotopic anomalies of rare gases in the Nigorikawa geothermal area; evidence of mass fractionation.

The localities and the description of samples used in this Section have been described in SectionIII-2e. Samples used are bubble gas Ll-NG and five soil gases Sl-NG-1 ~ Sl-NG-5.

Isotopic compositions of Ne and Ar are shown in Fig.III-7 and Fig. III-8 with delta values defined by Eq. III-4. A mass fractionation line through tha atmospheric value is defined by Eq. III-3. In Fig. III-7, the data fit a mass fractionation line of atmospheric Ne and Ar. As given in Table III-1, the most fractionated sample Sl-NG-4 has a $^{22}Ne/^{20}Ne$ ratio of 0.0968 ± 0.0009, more than 5 % enrichment in ^{20}Ne relative to the atmospheric ratio. This sample also shows the lowest $^{38}Ar/^{36}Ar$ ratio of 0.179 ± 0.002, enrichment in ^{36}Ar by more than 4% relative to atmospheric Ar. Such a correlation plot was not applicable to $^{21}Ne/^{20}Ne$ ratio because of relatively large experimental uncertainties mentioned in Section II-3. Fig. III-8 shows a correlation diagram of $^{40}Ar/^{36}Ar$ against $^{38}Ar/^{36}Ar$. The enrichment in the light isotopes of Ar is also well expressed by the mass fractionation line with a slope of 1.95 given by Eq. III-3 except for a high $^{40}Ar/^{36}Ar$ ratio of 325 ± 7 in sample Ll-NG, which is due to an addition of radiogenic ^{40}Ar. The isotopic correlation given in Fig. III-7 and Fig. III-8 indicates that the isotopic anomalies of Ar in the present samples can be

attributed to a mass fractionation process. At present, we cannot specify the mechanism for the mass fractionation process which produced the observed isotopic variation. However, it is noted that a single step of the Rayleigh process cannot produce as great a mass fractionation in Ne and Ar as was found in samples S1-NG-1 and S1-NG-4. For the most fractionated samples S1-NG-1 and SL-NG-4, K(X)'s,the mass fractionation per fractional mass difference defined by Eq. III-3 are listed in Table IV-1. Ar is more fractionated than Ne, as can be seen in Table IV-1.

The isotopic compositions of Kr and Xe in samples S1-NG-1 and S1-NG-4 which contain the most fractionated Ne and Ar are represented in Fig. III-9a and Fig. III-9b. The systematic enrichment in the light isotopes of Kr and Xe found in Fig. III-9a and Fig. III-9b supports the above-mentioned conclusion that a mass dependent process is responsible for the isotopic variations of Ne and Ar in the soil gas samples.

Fig. III-10 shows an elemental fractionation patterns defined by Eq. III-5 for the Nigorikawa gases. Sample L1-NG is highly enriched in He but has the elemental abundance pattern classified type-1 by Ozima and Alxander[60] for the other four gases. Samples S1-NG-2, S1-NG-3 and S1-NG-5 have almost the atmospheric elemental composition except for He. Samples S1-NG-1 and S1-NG-4 are enriched in He and Ne, and depleted in Kr and Xe relative to Ar. This elemental abundance pattern can be interpreted as the mass fractionation of atmospheric rare gas plus the admixture of mantle He with a high $^{3}He/^{4}He$ ratio. It is clear that the fractionation of isotopic compositions of Ne and Ar is well correlated with the fractionation of the elemental composition except for sample L1-NG. Sample L1-NG shows a slight enrichment in the light isotopes of

Ne and Ar. The elemental abundance pattern in this sample is progressively depleted in the light elements except for He, while the fractionation trend in the soil gas samples is the systematic enrichment in both light isotopes and light elements. This difference between sample L1-NG and other soil gases may represents the different origin of these gases.

A remaining problem about the material balance in the mass fractionation process should be investigated in future work.

In conclusion, mass fractionated rare gases were first observed in soil gas samples from the Nigorikawa geothermal area. This means that several per cent enrichment in ^{20}Ne relative to ^{22}Ne, which was usually regarded as evidence for primordial Ne[e.g.27], can be produced by the mass fractionation of atmospheric Ne in the crust and thus it is not a sufficient condition for identifying a primordial component of Ne in the earth.

4) Ne in volcanic gases.

As described in Section III-3, Ne in volcanic gases shows an isotopic variation. Fig. III-7 shows an isotopic anomaly of Ne in volcanic gases. The $^{22}Ne/^{20}Ne$ ratio estimated for the volcanic Ne is 0.100 ± 0.001, 20 per mil lower than the atmospheric ratio of 0.1020.

Isotopic variations of terrestrial Ne attributable to nuclear reactions in rocks and minerals have been reported by several workers and summarized by Tolstikhin[74]. Principal nuclear reactions responsible for the isotopic variations of Ne in the earth are (α, n) and (n, α) reactions on isotopes ^{17}O, ^{18}O, ^{19}F and ^{25}Mg where α-particles originate from α-decays of U and Th, and neutrons are produced by the (α, n) reactions on environmental rocks. The

$^{17}O(\alpha, n)^{20}Ne$ reaction gives a low $^{22}Ne/^{20}Ne$ ratio. But the parallel reaction $^{18}O(\alpha, n)^{21}Ne$ is to produce an isotopic anomaly at ^{21}Ne. Such a ^{21}Ne excess has not been found in the present samples, however. On the other hand, Craig and Lupton[27] have estimated that the change in the $^{22}Ne/^{20}Ne$ ratio in the earth's atmosphere caused by an addition of ^{22}Ne produced by the $Mg(n, \alpha)$ reaction in crustal rocks is at most 2 per mil. This is an order of magnitude less than the observed isotopic variation. Hence the nuclear reactions cannot explain the isotopic variation in volcanic Ne.

An alternative explanation of the low $^{22}Ne/^{20}Ne$ ratio is emanation of a primordial component of Ne. Low $^{22}Ne/^{20}Ne$ ratios relative to the atmospheric values have been found in ancient rocks [75], thermal fluids[76], Kilauea gas and submarine basalts[27] and amphibole[32]. Craig and Lupton[27] attributed the enrichment in ^{20}Ne to a solar-type primordial Ne emanation. However, since they have not measured the isotopic composition of other rare gases than He and Ne, the mass fractionation effect cannot be corrected using the correlation plot used in this work. Low $^{22}Ne/^{20}Ne$ and $^{38}Ar/^{36}Ar$ ratios relative to the atmospheric values found in amphibole[32] lie on the mass fractionation line through the atmospheric point within experimental errors. This suggests that the low ratios resulted from the mass fractionation of atmospheric Ne and Ar in amphibole. In contrast to amphibole and the Nigorikawa soil gases, the isotopic ratios of Ne and Ar in the volcanic gas samples, as shown in Fig. III-7, cannot result from the mass fractionation of atmospheric Ne and Ar defined by the mass fractionation line through the atmospheric point.

If the low $^{22}Ne/^{20}Ne$ ratio found in volcanic Ne is due to admixture of solar type Ne ($^{22}Ne/^{20}Ne = 1/13$) with atmospheric Ne

($^{22}Ne/^{20}Ne$ = 1/9.80), the solar-type component amounts to several per cent of Ne. Whether such primordial Ne still remains in the volcanic gases or not is a very interesting problem to be clarified.

If atmospheric Ne as well as He has escaped from the upper atmosphere to the inter-planetary space, the isotopic effect on the escape rate could change the $^{22}Ne/^{20}Ne$ ratio in the atmosphere. When a mass-dependent diffusive loss of atmospheric Ne is considered, the Rayleigh equation predicts 34% defficiency of initial Ne to increase the $^{22}Ne/^{20}Ne$ ratio from 0.100 to the present value of 0.102.

Whereas the thermal escape from the exosphere is considered, the escape rate is calculated by[77],

$$F(r) = n(r, m) \left(\frac{g(r)}{2\pi}\right)^{1/2} r\, H(r)^{-1/2} \exp\left(-\frac{r}{H(r)}\right) \quad (\text{Eq. IV-2})$$

where "r" is a distance from the center of the earth to the exosphere, n(r, m) is the number density of isotope "m" at the exosphere and g(r) is the gravitational accelaration at "r". H(r) is the scale hight at "r" defined by H(r) = kT/mg(r), where "k" is the Boltzmann constant, "m" mass of the isotope and "T" temperature of the neutral atmosphere at "r". The ratio of escape rates between ^{20}Ne and ^{22}Ne can be deduced from Eq. IV-2 as,

$$\frac{F_{20}}{F_{22}} = \frac{n(r, 20)}{n(r, 22)} \left(\frac{20}{22}\right) \exp\left\{\frac{r\, g(r)}{k\, T} (m_{22} - m_{20})\right\} \quad (\text{Eq. IV-3})$$

With the atmospheric ratio of about 0.1 for n(r, 22)/n(r, 20) ratio, the ratio of escape rate F_{20}/F_{22} at the altitude of 500 to 1,000 km varies from 100,000 to 300 according as temperature from 1,500K to 4,000K. This requires the Ne loss of at most 2% of initial Ne to increas the $^{22}Ne/^{20}Ne$ ratio from 0.100 to 0.102. However, the

calculated escape rate by Eq. Ⅳ-2 with Ne number density of less than 10^4 atoms cm^{-3} [78] is too small to explain the 2% defficiency of Ne on the same condition of temperature and altitude used above. Hence the thermal escape of Ne requires some extreme condition such as very high temperature at exosphere.

The origin of isotopically anomalous Ne in volcanic gases is not conclusive.

5) Isotopic composition of Ar.

The $^{40}Ar/^{36}Ar$ ratio for primordial Ar has been calculated to be 2×10^{-4} based on nucleosynthetic theory[7]. The ratio in the present earth's atmosphere is 295.5. The increase in $^{40}Ar/^{36}Ar$ ratio is attributed to degassing of radiogenic ^{40}Ar from the solid earth. Since the ^{40}Ar concentration in the earth's interior depends on the K concentration and degassing rate, the $^{40}Ar/^{36}Ar$ ratio in the deep interior of the earth offers important information about the origin and evolution of earth's atmosphere. Based on the $^{40}Ar/^{36}Ar$ ratio in the mantle, Ozima[8] proposed a catastrophic degassing of volatiles from the mantle at the early stag- of the earth's evolution.

In gas samples plotted in Fig. Ⅲ-8, $^{40}Ar/^{36}Ar$ ratios range from atmospheric value of 295.5 to 325 except for mass fractionated Ar. These ratios are much lower than the high ratios found in continental CO_2 well gas ($^{40}Ar/^{36}Ar$ = 845 in DR63) and Mid-Atlantic ridge basalt ($^{40}Ar/^{36}Ar$ = 451 in RB197). Such relatively small ^{40}Ar excess can be understood as the large atmospheric Ar contamination. Hence the sufficient information about the $^{40}Ar/^{36}Ar$ ratio in the upper mantle beneath the Japanese Islands can not be derived from the $^{40}Ar/^{36}Ar$ ratios in gas samples analyzed in this work.

$^{40}Ar/^{36}Ar$ ratios lower than the atmospheric value of 295.5 have been reported in lava flows[79], volcanic rocks[80] and CO_2-rich soil gases[61]. Krummenacher[80] showed first that the mass fractionation effect was responsible for the low $^{40}Ar/^{36}Ar$ ratios in volcanic rocks. Nagao et al.[61] also showed that the low $^{40}Ar/^{36}Ar$ ratios in soil gas samples were accompanied with low $^{38}Ar/^{36}Ar$ ratios due to the mass fractionation. (in Section Ⅳ-3)

The data for volcanic lava and gas samples given in Fig. Ⅲ-8 confirm the mass fractionation model. Three gas samples Hl-IW, V2-SS-6 and V9-SI-1 as well as the Nigorikawa gas samples lie on the fractionation line within experimental errors. Ar in volcanic lava VL-IO, VL-NS and VL-HY also show large depletions in ^{40}Ar and lie on the fractionation line. Low $^{40}Ar/^{36}Ar$ ratios in Japanese volcanic lava were reported by Dalrymple[79], the ratios of which were 293.7 and 291.4 for lava from Mt. Mihara and Mt. Sakurajima, respectively. Although these data include no $^{38}Ar/^{36}Ar$ ratios, the low $^{40}Ar/^{36}Ar$ ratios may be due to the mass fractionation. Though a mechanism for the mass fractionation of atmospheric Ar is not clear, these data show that such mass fractionated Ar in volcanic lava and in gas samples seems to be not uncommon. A single step of the Rayleigh process for a mass fractionation of atmospheric Ar gives lower limit of $^{40}Ar/^{36}Ar$ ratio to be 281, corresponding to $\delta(40/36) = 51.3$ per mil. In samples Sl-NG-1, Sl-NG-4, and 1800°C fractions for samples VL-NS and VL-HY, $^{40}Ar/^{36}Ar$ ratios were lower than this limit. This means that we have to consider more complicated mechanisms for the low $^{40}Ar/^{36}Ar$ ratios such as a multi-step Rayleigh process.

6) Elemental abundances of rare gases.

Elemental abundance patterns are shown in Fig. III-10. As noted in Section III-5, the abundance patterns are similar to that of atmospheric rare gases dissolved in water.

Matsubayashi et al.[38] have shown that the elemental abundance patterns of fumarolic gases in Japanese volcanoes, Tokachi-dake, Showa-shinzan and Satsuma-Iwojima were between the atmospheric rare gases and the fractionated atmospheric rare gases dissolved in water. They explained these patterns to be the mixture of atmospheric rare gases with the fractionated atmospheric rare gases present in local low-temperature ground water.

This model, however, cannot be applicable to some volcanic gases such as V2-SS-1, V3-US and V5-HK, and other bubble samples L2-MC, H1-IW, L3-YS, H11-KY, H12-YN and L7-IK. These samples are more enriched in Kr and Xe relative to the atmospheric rare gas solubility into water. The enrichments in Kr and Xe suggest more complicated degassind processes for the gas samples.

One explanation to be considered for the heavy rare gas enrichments in the active volcano such as Mt. Usu is the addition of heavy rare gases released from the sedimentary materials on the subducting oceanic plate to the fractionated atmospheric rare gases dissolved in water. Same mechanism for enrichment in N_2 gas relative to Ar has been proposed by Matsuo et al.[37]. Another source of the heavy rare gases are calcareous rocks in crust from which they are released by a chemical reaction of hydrochloric acid from the magma as will be discussed in Section IV-8. The heavy rare gases are probably enriched in sedimentary materials[86]. This explanation seems to be applicable to CO_2-rich bubble samples noted above. These samples are enriched in heavy rare gases relative to atmospheric rare gas solubility into water.

Another explanation for the heavy rare gas enrichments in the active volcanic gases is that the elemental abundance pttern represents the rare gas composition in magma, because the elemental abundance pattern is similar to the rare gas composition discovered in mantle-derived materials[28, 29, 31, 32, 81].

Volcanic gas collected at the active volcano Mt. Usu in 1978 (V3-US), which showed most enrichment in Kr and Xe, and the samples V2-SS-1 and V2-SS-4 collected at Mt. Showa-shinzan in 1958 and 1964, respectively, suggest that a declination of volcanic activity is correlated with a reduction of heavy rare gas enrichment. This can be explained by the increasing atmospheric contamination dissolved in local water to magmatic gas as the volcanic activity declines. This explanation is also supported by the $^{3}He/^{4}He$ and $^{4}He/^{20}Ne$ ratios shown in Fig. Ⅲ-2.

7) Yearly change of rare gas composition in volcanic gas from Showa-shinzan.

Mt. Showa-shinzan volcano,located near Mt. Usu volcano,erupted in 1944 and is now emitting fumarolic gases.

Matsuo et al.[37] summarized the N_2/Ar ratios observed in fumarolic gases collected in various fumaroles of Mt. Showa-shinzan from 1954 to 1965. The ratios decreased with time from 2,200 in 1954 to 98 in 1965 according as the decreasing volcanic activity[37].

Variations in the isotopic and elemental compositions of rare gases investigated in this work are compatible with the result given by Matsuo et al.[37]. It has beenalready pointed out in Section Ⅳ-6 that the enrichment of Kr and Xe in the elemental abundance pattern decreased with the declination of volcanic activity.

Table Ⅳ-2 lists $^{3}He/^{4}He$ and $^{4}He/^{20}Ne$ ratios measured and

corrected for permeation of He through the glass wall of a sample vessel in storage time. Permeabilities of ^4He used for borosilicate glass# and Pyrex-glass were 1×10^{-13} and 2×10^{-12} cc mm cm^{-2} $Torr^{-1}$ sec^{-1} [82]. The permeability ratio of ^3He to ^4He was assumed to satisfy the following relation,

$$\frac{\xi_3}{\xi_4} = (M_4/M_3)^{1/2} \qquad \text{(Eq. Ⅳ-4)}$$

where ξ and M mean permeability and mass of He, respectively, and subscripts "3" and "4" mean ^3He and ^4He, respectively. The correction was negligibly small for borosilicate glass, while the correction for sample V2-SS-5 in a Pyrex-glass container lead to a very high $^3He/^4He$ ratio of 1.4×10^{-5}. Such high ratio for this sample is unreasonable because of the declination of volcanic activity as shown by the $^4He/^{20}Ne$ and the N_2/Ar ratios[37]. Hence the corrected ratios for V2-SS-5 and V2-SS-6 should be considered as an upper limit.

Sample V3-US collected on October 9, 1978 at Mt. Usu volcano is also listed in Table Ⅳ-2 for comparison. The $^3He/^4He$ and $^4He/^{20}Ne$ ratios are expected to reproduce those for Mt. Showa-shinzan at the early stage of eruption, which was supported by similarity in the chemical composition between fumarolic gases from Mt. Usu and from Mt. Showa-shinzan at the early stage of eruption[40].

The $^3He/^4He$ ratios from C-2 and C-3 fumaroles in 1959 are similar to those from A-1 fumaroles before 1974, and the N_2/Ar ratios from fumaroles A-1, C-2 and C-3 in 1959 were also similar, 302, 328 and 353, respectively[37]. However the $^4He/^{20}Ne$ ratios from C-2

SB-glass by Shibata glass factory.

and C-3 fumaroles were significantly low relative to those for A-1 fumarole. Because of the similarity in both the N_2/Ar and $^3He/^4He$ ratios among these fumaroles, the low $^4He/^{20}Ne$ ratios for C-2 and C-3 fumaroles are due not to atmospheric contamination but to the low He concentration in C-2 and C-3 fumaroles.

The $^3He/^4He$ and $^4He/^{20}Ne$ ratios except the $^4He/^{20}Ne$ ratios for C-2 and C-3 fumaroles have decreased with time and approached to the atmospheric values. Such a decrease is consistent with the result on the N_2/Ar ratio[37]. The observed decrease in the $^3He/^4He$ and $^4He/^{20}Ne$ ratios can be explained by exhaustion of primordial He in magma. The low $^3He/^4He$ and $^4He/^{20}Ne$ ratios in samples collected in 1974 and 1977 suggest the declination of volcanic activity of Mt. Showa-shinzan. Sample V2-SS-7 was collected in 1977, immediately after the eruption of Mt. Usu volcano. There was no sign of increase in the $^3He/^4He$ ratio in this sample. From this we can conclude no connection now with respect to rare gases between the two volcanoes. The fumarolic gas in Mt. Showa-shinzan is not supplied from a deep seated magma but supplied from a relatively shallow and small volume of magma beneath Mt. Showa-shinzan.

8) $^3He/^4He$ ratio: a possible candidate for the detection of earthquake precursors.

The detection of earthquake precursors is not only interesting in a scientific aspect, but also important to the earthquake prediction. The earthquake prediction is one of the present-day social requisites to science. Various geophysical and geochemical methods are being applied to detect earthquake precursors. Methods for the detection of earthquake precursors, however, have not been established to date because of the lack of sufficient knowledge about the earthquake

mechanism, and because of the lack of sufficient observations of phenomena accompanied with the earthquake.

Geochemical methods as well as geophyscal ones are considered to be usefull for the detection of precursory changes prior to an earthquake. For example, the change of Rn and He concentrations in ground water have been reported[13].

Sugisaki[83] reported the change of He/Ar and N_2/Ar ratios in gas samples collected on a fault prior to some earthquakes, and attributed the change to the release of lithospheric gases expelled by the stress in rocks before the earthquakes. The He/Ar and N_2/Ar ratios in the lithosphere are considered to be higher than the atmospheric ones because of the presence of radiogenic ^{4}He and ^{40}Ar, and of the decomposition of nitrogen-bearing compounds. Sugisaki [83] also suggested that the concentrations of rare gases can be easily changed by an admixing of other gases such as CH_4 and CO_2 formed in the ground, so the ratios of He/Ar and N_2/Ar are more reliable indicators ofprecursory phenomena.

In this Section, it will be shown that the isotopic composition of He may be a useful measure for the detection of earthquake precursors. The Matsushiro earthquake swarm occured during 1965 to 1967. Detailed description of the phenomena have been reported elsewhere [84]. Initially the earthquake foci were centered beneath the Mt. Minakami andesitic dome, and gradually spread in a northeast to southwest direction, and a fault was formed along this direction. More than 600 felt earthquakes occured in a day at the most active period. Large amount of ground water of about $10^7 m^3$ with an anomalous chemical composition was gushed at the fault region. There the gases enriched in CO_2 and in N_2 were emitted after the earthquake swarm.

In 1975, about ten years after the earthquakes, Wakita et al. [36] began to investigate the emitting gases to estimate the degree of the fault activity and to get information for earthquake prediction and for the assessment of the He budget for the earth-atmosphere system. Analyses of chemical compositions with a helium leak detector and a gas chromatograph indicated a high He concentration of about 300 ppm in N_2-rich gas sample. The concentration of He in CO_2-rich gas was about 5 ppm, identical to the atmospheric one. Estimation of He flux at the fault region was about 3×10^{10} atoms cm^{-2} sec^{-1}, which was significantly higher than the average crustal production rate of about 10^6 atoms ^4He cm^{-2} sec^{-1} [85].

This discrepancy was solved by the isotopic analyses of rare gases in 1977. Unexpectedly high $^3He/^4He$ ratios, about 6.5 times the atmospheric ratio, were discovered by measuring the isotopic composition of He in those two gas samples with a high-sensitivity, rare gas mass spectrometer at Department of Physics, Osaka University. One of the samples consisted of 80%N_2 and 20%CO_2 including about 300ppmHe and another consisted of 7%N_2, 93%CO_2 and about 5ppmHe[36]. The observed high $^3He/^4He$ ratio showed that He in these gas samples collected on the earthquake fault was not crustal He supplied by the α-decay of U and Th but mantle-derived He enriched in ^3He. This result lead to the idea of "a diapiric magma" from the upper mantle as a cause of the Matsushiro earthquake swarm[36]. Volatiles in the diapiric magma were excluded from the crystalizing magma and emitted into the surface through the fault region.

Isotopic compositions of rare gases summarized in TableIII-1 are the averaged values of the additional several analyses. Hence the $^3He/^4He$ ratio slightly differs from the ratio quoted by Wakita et al.[36]. The isotopic ratios except $^3He/^4He$ and $^{40}Ar/^{36}Ar$ were

atmospheric within experimental errors. The $^{40}Ar/^{36}Ar$ ratio was higher than that of atmospheric Ar and is similar to the $^{40}Ar/^{36}Ar$ ratio found in various types of gas samples collected in the Japanese Islands as described earlier.

Elemental abundance patterns for both samples belong to type-1 [60] as shown in Fig. III-10. This type of elemental abundance pattern is common in gas samples collected in the Japanese Islands. A comparison between the abundance patterns for two gas samples shows that He and Ne are depleted in the CO_2-rich gas and Kr and Xe are enriched relative to the N_2-rich gas. As noted in Section III-2d, the He content in the CO_2-rich gas is much lower than that in the N_2-rich gas.

The diapiric magma model[36] also suggested that the CO_2 gas might be produced by a chemical reaction of hydrochloric acid from the magma with calcareous rock in the crust. With this model, the low He concentration in the CO_2-rich gas could be attributed to dilution of He-rich magmatic gas with the CO_2 gas produced in the crust. This mechanism may also produce the enrichment of heavy rare gases found in CO_2-rich gas sample L2-MC because of an admixture of rare gases released by the chemical reaction. The heavy rare gas enrichment in sedimentary materials can be suggested by the elemental abundance pattern in Fig Tree Shale[86]. Heavy rare gases such as Kr and Xe are more adsorptive relative to the light rare gases.

In spite of the difference in the chemical composition between the two samples, the $^{3}He/^{4}He$ ratios for both of the samples were identical. This means the same origin of He in both of the samples and the negligibl atmospheric and crustal He contamination despite

an admixing CO_2 gas produced by the chemical reaction mentioned above.

The presence of mantle He in the gas emanation first discovered at the earthquake fault in Matsushiro strongly suggests that the isotopic composition of He is a useful measure for the detection of earthquake precursors. As already described, mantle He occurs ubiquitously in gas samples in the Japanese Islands. This fact means that the mantle He with a high $^3He/^4He$ ratio is easily emitted through the cracks in crustal rocks at a fault region. Such a high $^3He/^4He$ ratio can be easily detected because of the low abundance of atmospheric He. It is expected that the continuous analyses of He isotopic ratio as well as the concentration of He in soil gas and naturally bubbling gas at the fault region provide a method to detect an earthquake precursor, because many cracks in crustal rocks around a focal region are developed by the increasing stress, from which He can be released. It is difficult to estimate the contribution of crustal He enriched in ^4He released from deformation of crustal rocks prior to an earthquake to the mantle He emanation. How the $^3He/^4He$ ratio changes in naturally-occuring gas and liquid samples before and after an earthquake depends on the mixing ratio of the crustal He to the mantle He. A suggestion for this can be given by the hot-spring gases collected at Matsue and Shramine, both of which were drilled recently. The high He concentration and relatively low $^3He/^4He$ ratios in these samples suggest the large contribution of radiogenic ^4He accumulated in the surrounding crustal rocks. From this fact it is expected that at first the $^3He/^4He$ ratio decreases from the average value because of possible release of crustal He from circumstanced rocks under the increasing stress.

As already described in this Section, Sugisaki[83] assumed that

the observed high He/Ar ratio compared with the atmospheric value ($He/Ar = 5.7 \times 10^{-4}$) was owing to a crustal rare gas contribution based on a theoretical production ratio of radiogenic ^4He to radiogenic ^{40}Ar in common crustal rocks($^4He/^{40}Ar \sim 10$). For the gas samples S2-MN and L2-MC collected in Matsushiro, the He/Ar ratios observed are higher than 0.016, more than 30 times the atmospheric ratio and the $^3He/^4He$ ratios are 6.5 times the atmospheric $^3He/^4He$ ratio. He with the high $^3He/^4He$ ratio is not of the crustal origin but of the mantle origin. Therefore, if the origin of He is not identified, only the high He/Ar ratio observed may lead to an erroneous interpretation about the origin of He. As shown in Table III-1, gases with high He/Ar and $^3He/^4He$ ratios relative to the atmospheric values are common in Japanese natural gases.

In conclusion, He with high $^3He/^4He$, 6.5 times the atmospheric ratio, was first observed in gas samples emanated at the earthquake fault region in Matsushiro. The observed high $^3He/^4He$ ratio was attributed to the emanation of primordial mantle He.

ontinuous observation of He isotopic composition may provide useful measure for the detection of precursory change prior to an earthquake.

9) Heat source of hot-spring.

High $^3He/^4He$ ratios were observed in all Japanese hot-spring gases analyzed to date. As mentioned previously the high $^3He/^4He$ ratio can be explained as a contribution of primordial He remaining in the mantle. Therefore the observed He is the first direct evidence for a juvenile volatile emanation in Japanese hot-springs.

Some mechanisms for the heat transfer from a magmatic heat source to ground water were proposed to explain the heat flow of hot-spring. One model was a conductive heat transfer from a high temperature

igneous rock and magma. High heat flow rate greater than $10^{8.5}$ cal/min cannot be explained unless the magmatic high temperature water vapor or liquid was directly supplied to ground water[87]. High $^{3}He/^{4}He$ ratios observed in all hot-spring gases analyzed suggest that the magmatic volatiles are also supplied into ground water accompanied with He. This means that magmatic water is supplied to ground water to some extent as a heat transport in all hot-springs. Such volatiles should be emitted from a deep seated magma through faults and cracks. In comparison with the relatively short age of Mt. Showa-shinzan with respect to the $^{3}He/^{4}He$ ratio as noted in Section Ⅳ-7, long period of mantle He emanation in hot-springs indicates that the heat sources are large and deep relative to that for Mt. Showa-shinzan.

V. Conclusion.

1) He in gas samples collected in the Japanese Islands showed significantly high $^3He/^4He$ ratios of about 7 times the atmospheric ratio of 1.4×10^{-6} in spite of the large variation of He concentration. Such high ratios were consistent with the $^3He/^4He$ ratios observed in circum-Pacific volcanic gases by Craig et al. [18] and in volcanic gases from the Kamchatka Peninsula by Kamenskiy et al.[16]. Those ratios were relatively lower than the ratios observed in Mid Atlantic oceanic basalts[27], Kilauea volcanic gas[27], mantle-derived minerals[28-32]. This suggests a relatively large radiogenic ^4He contribution to the mantle He in the subducting zone.

He in volcanic gas, hot-spring gas, geothermal well gas and most of bubble gas in low temperature water pool showed no systematic difference in the $^3He/^4He$ ratios. He in those samples consisted mainly of mantle He enriched in primordial He and contain a minor component of radiogenic ^4He. An emanation of He with the high $^3He/^4He$ ratio is ubiquitous in the Japanese Islands.

2) Ne in volcanic gases showed the $^{22}Ne/^{20}Ne$ ratio about 2 per cent lower than the atmospheric ratio. The anomaly in $^{22}Ne/^{20}Ne$ ratio can not produced by the mass fractionation of the atmospheric Ne. The origin of such low $^{22}Ne/^{20}Ne$ ratio in volcanic gas samples has not been clarified and further investigation on the isotopic composition of Ne in volcanic gas is required.

3) Isotopic compositions of Ar in most of samples were explained in terms of the mixture of atmospheric Ar and radiogenic ^{40}Ar.

The contribution of radiogenic ^{40}Ar was relatively small in gas samples collected in the Japanese Islands.

Ar in volcanic lava and soil gas samples showed systematic enrichment in light isotopes, which could be explained as a mass fractionation of atmospheric Ar.

4) Soil gas samples collected in the Nigorikawa geothermal area, Hokkaido, showed evidence for the mass fractionation of the atmospheric rare gases in the isotopic compositions of Ne, Ar, Kr and Xe, and in the elemental abundances. This means that several per cent enrichment of ^{20}Ne relative to ^{22}Ne, which wasusually regarded as evidence for primordial Ne, can be produced by the mass fractionation of atmospheric Ne in the crust and thus it is not a sufficient condition for identifying a primordial component of Ne in the earth.

5) Elemental abundance patterns in gas samples were similar to type-1 pattern classified by Ozima and Alexander[60], which was interpreted as the fractionation established by the low temperature solubility into water. He was enriched in all samples studied relative to the atmospheric composition.

More enrichments in Kr and Xe relative to the atmospheric rare gas solubility into water for some samples could be explained by the release of heavy rare gases from sedimentary materials or calcareous rocks. Another explanation was that the abundance patterns represent the rare gas composition in magma.

6) $^{3}He/^{4}He$ and $^{4}He/^{20}Ne$ ratios in volcanic gases from shinzan decreased and approached to the atmospheric values with

time. This suggests the declination of volcanic activity of Mt. Showa-shinzan. Samples collected at Mt. Showa-shinzan immediately after the eruption of Mt. Usu volcano in 1977 showed no sign of increase in the $^{3}He/^{4}He$ ratio, which indicates no connection with respect to rare gases between the two volcanoes.

7) High $^{3}He/^{4}He$ ratios were first observed in gas samples collected at the earthquake fault zone in the Matsushiro earthquake swarm. This strongly suggests that the isotopic composition of He is useful measure for the detection of earthquake precursors.

8) High $^{3}He/^{4}He$ ratios observed in all hot-spring gases collected in the Japanese Islands suggest that the magmatic volatiles are also supplied into ground water to some extent as a heat transport in all hot-springs.

Acknowledgements.

I wish to express my grateful thanks to Professor Nobuo Takaoka of Yamagata University for his constant guidance and invaluable advice in the course of this work. Sincere gratitude is also expressed to Professor Koreichi Ogata of Okayama University of Science for introducing me to this field of mass spectrometry. My grateful thanks are expressed to Mr. Osamu Matsubayashi of Geological Survey of Japan. He provided some of gas samples and took part in collection of samples. Thanks are also expressed to Mr. Masahiko Honda of Tokyo University who took part in the experiment on ridge basalts and volcanic lava. I am grateful to Professors Sadao Matsuo of Tokyo Institute of Technology, Yoshihiko Mizutani of Nagoya University and Hiroshi Wakita of Tokyo University, and Mr. Yoshio Uyeda of Maritime Safety Agency for kindly providing samples. I thank Professor Minoru Ozima of Tokyo University for his valuable suggestions and careful review of this manuscript. I am also grateful to Dr. Ichiro Kaneoka of Tokyo University for fruitful discussions of the problems which arose in this work. Grateful thanks are expressed to many people for their generous assistances in collection of gas samples.

References

1) H. Brown, Rare gases and the formation of the Earth's atmosphere, *in* Atmosphere of the Earth and Planets, 2nd ed., pp 258-266, Univ. Chicago Press, Chicago, 1952.

2) W. W. Rubey, Geologic history of sea water, Bull. Geol. Soc. Am., 62, (1951) 1111.

3) K. K. Turekian, Degassing of argon and helium from the earth, *in* The Origin and Evolution of Atmosphere and Oceans, ed. P. J. Brancazio and A. G. W. Cameron, pp 74-82, Wily, 1964.

4) M. Ozima and K. Kudo, Excess argon in submarine basalts and an earth-atmosphere evolution model, Nature Phys. Sci., 239, (1972) 23-24.

5) F. P. Fanale,A case for catastrophic early degassing of the earth, Chem. Geol., 8, (1971) 79-105.

6) D. W. Schwartzman, Ar degassing and the origin of the sialic crust,-Geochim. Cosmochim. Acta, 37, (1973) 2479-2495.

7) A. G. W. Cameron, Abundaces of the elements in the solar system, Space Sci. Rev., 15, (1973) 121-146.

8) M. Ozima, Ar isotopes and earth-atmosphere evolution models, Geochim. Cosmochim. Acta, 39, (1975) 1127-1134.

9) M. S. Boulos and O. K. Manuel, The xenon record of extinct radioactivities in the earth, Science, 174,(1971) 1334-1336.

10) E. W. Hennecke and O. K. Manuel, Noble gases in CO_2 well gas, Harding County, New Mexico, Earth Planet. Sci. Lett., 27, (1975) 346-355.

11) E. W. Henneke and O. K. Manuel, Noble gases in lava rock from Mount Capulin, New Mexico, Nature, 256,(1975) 284-287.

12) E. W. Henneke and O. K. Manuel, Noble gases in an Hawaiian xenolith, Nature, 275,(1975) 778-780.

13) see references quoted by Wakita, *in* Geochemistry as a tool for earthquake prediction, in Earthquake Precursors, ed. C. Kisslinger and Z. Suzuki, pp. 175-183, Cent. Acad. Publ. Japan, Tokyo,1978.

14) I. Kaneoka, N. Takaoka, Excess ^{129}Xe and high $^{3}He/^{4}He$ ratios in olivine phenocrysts of Kapuho lava and xenolithic dunites from Hawaii, Earth planet. Sci. Lett., 39, (1978) 382-386.

15) Reviewed by K. Rankama, in Isotope Geology, ed. K. Rankama, pp.161-175, London Pergamon Press Ltd. 1954.

16) I. L. Kamenskiy, A. Lobkov, E. M. Prasolov, N. S. Beskrovnyy, E. I. Kudryavtseva, G. S. Anufriyev and V. P. Pavlov, Components of the upper mantle in the volcanic gases of Kamchatka (according to He, Ne, Ar, and C isotopy) Trans. from Geokhimiya, No. 5, pp. 682-694, (1976).

17) B. A. Mamyrin, I. N. Tolstikhin, G. S. Anufriyev and I. L. Kamenskiy, Abnormal isotopic composition of helium in volcanic gases, Trans. from Doklady Akademii Nauk USSR, 184,(1969) 1197-1199.

18) H. Craig, J. E. Lupton and Y. Horibe, A mantle helium component in circum-Pacific volcanic gases: Hakone, the Mariana, and Mt. Lassen, in Terrestrial Rare Gases, ed. E. C. Alexander, Jr. and M. Ozima, pp.3-16, Cent. Acad. Publ. Japan, Tokyo, 1978.

19) H. Craig, J. E. Lupton, J. A. Welhan and R. Poreda, Helium isotope ratios in Yellowstone and Lassen Park volcanic gases, Geophys. Res. Lett., 5, (1978) 897-900.

20) W. B. Clarke, M. A. Beg and H. Craig, Excess ^{3}He in the sea: evidence for terrestrial primordial helium, Earth Planet Sci. Lett., 6, (1969) 213-220.

21) W. B. Clarke, M. A. Beg and H. Craig, Excess helium 3 at the North pacific Geosecs Station, J. Geophys. Res., 75,(1970) 7676-7678.

22) J. E. Lupton, The ^{3}He distribution in deep water over the Mid-Atlantic Ridge, Earth Planet. Sci. Lett., 32, (1976) 371-374.

23) J. E. Lupton, R. F. Weiss and H. Craig, Mantle helium in hydrothermal plumes in the Galapagos Rift, Nature, 267,(1977) 603-604.

24) J. E. Lupton, R. F. Weiss and H. Craig, Mantle helium in the Red Sea brines, Nature, 266, (1977) 244-246.

25) A. Ta. Krylov, B. A. Mamyrin, L. A. Khabarin, T. I. Mazina and Tu. I. Silin, Helium isotopes in oceanic-floor bedrock, Trans. from Geokhimiya No. 8, (1974) 1220-1225.

26) J. E. Lupton and H. Craig, Excess ^{3}He in oceani basalts: evidence for terrestrial primordial helium, 26, (1975) 133-139.

27) H. Craig and J. E. Lupton, Primordial neon, helium and hydrogen in ocenic basalts, Earth Planet. Sci. Lett., 31, (1976)369-385.

28) N. Takaoka and M. Ozima, Rare gas isotopic composition in diamonds, in Terrestrial rare rases, ed E. C. Alexander, Jr.•and M. Ozima, pp. 65-70, Cent. Acad. Publ.Japan, Tokyo, 1978.

29) N. Takaoka and M. Ozima, Rare gas isotopic compositions in diamonds, Nature, 271, (1978) 45-46.

30) I. N. Tolstikhin, B. A. Mamyrin, L. B. Khabarin and E. N. Erlikh, Isotope composition of helium in ultrabasic xenoliths from volcanic rocks of Kamchatka, Earth Planet. Sci. Lett., 22,(1974) 75-84.

31) I. Kaneoka, N. Takaoka and K. Aoki, Rare gases in mantle-derived rocks and minerals, in Terrestrial Rare Gases, ed. E. C. Alexander, Jr. and M. Ozima, pp. 71-83, Cent. Acad. Publ. Japan, Tokyo,1978.

32) K. Saito, A. Basu and E. C. Alexander, Jr., Planetary-type rare gases in an upper mantle-derived amphibole, Earth Planet. Sci. Lett., 39, (1978) 274-280.

33) P. M. Jeffery and E. Anders, Primordial noble gases in separated meteoritic minerals-I., Geochim. Cosmochim. Acta, 34,(1970)1175-1198.

34) D. C. Black, On the origin of trapped helium, neon and argon isotopic variations in meteorites - I. Gas-rich meteorites, lunar soil, and breccia, Geochim. Cosmochim. Acta, 36, (1972) 347-375.

35) D. C. Black, On the origins of trapped helium, neon and argon isotopic variations in meteorites - II. Carbonaceous meteorites, Geochim. Cosmochim. Acta, 36, (1972) 377-394.

36) H. Wakita, N. Fujii, S. Matsuo, K. Notsu, K. Nagao and N. Takaoka, "Helium Spots": caused by a diapiric magma from the upper mantle, Science, 200, (1978) 430-432.

37) S. Matsuo, M. Suzuki and Y. Mizutani, Nitrogen to argon ratio in volcanic gases, *in* Terrestrial Rare Gases, ed. E. C. Alexander, Jr. and M. Ozima, pp. 17-25, Cent. Acad. Publ. Japan, Tokyo, 1978.

38) O. Matsubayashi, S. Matsuo, I. Kaneoka and M. Ozima, Rare gas abundance pattern of fumarolic gases in Japanese volcanic area, *in* Terrestrial Rare Gases, ed. E. C. Alexander, Jr. and M. Ozima, pp. 27-32, Cent. Acad. Publ. Japan, Tokyo, 1978.

39) N. Takaoka, A low-blank metal system for rare gas analysis, Mass Spectroscopy, 24, (1976) 73-86.

40) S. Matsuo (1978) private communication.

41) N. Yamada, Bull. Chem. Soc. Japan, 43,(1922) 885-895.

42) N. Yamada, Bull. Chem. Soc. Japan, 44,(1923) 1018-1027.

43) B. Yamaguchi and Y. Kano, Bull. Chem. Soc. Japan, 47, (1926) 13-19.

44) B. Yamaguchi and Y. Kano, Bull. Chem. Soc. Japan, 47, (1926) 452-454.

45) I. Suganuma and K. Kitaoka,(1935) 239-296.

46) S. Maki, S. Nagata, T. Koma and T. Nemoto, Bull, Geol. Survey Japan, 22, (1971) 227-243.

47) S. Maki, K. Yazaki, T. Hirukawa and H. Yonetani, Bull. Geol. Survey Japan, 17, (1966) 695-715.

48) S. Maki, K. Motojima, M. Sasaki, T. Hirukawa, S. Nagata and K. Kageyama, Bull. Geol. Survy Japan, 21,(1970) 309-325.

49) S. Maki, K. Motojima, M. Sasaki, H. Kawachi, T. Hirukawa, H. Yonetani and S. Nagata, Bull. Geol. Survey Japan, 23,(1972) 349-363.

50) H. Yonetani and M. Miyashita , Bull. Geol. Survy Japan, 19, (1968) 717-724.

51) N. Ando, T. Otsuka and S. Nagata, Bull.Geol. Survey Japan, 19, (1968) 773-781.

52) S. Maki, K. Motojima, T. Hirukawa, H. Yonetani, T. Imai, T. Moritani, T. Otsuka and Y. Takeda, Bull. Geol. Survey Japan, Bull. Geol. Survey Japan, 25, (1974) 331-348.

53) K. Motojima, K. Shibata, M. Miyamura and T. Abe, Bull. Geol. Survey Japan, 20,(1969) 329-342.

54) N. Imai, M. Miyamura and S. Maki, Bull. Geol. Survey Japan, 18, (1967) 289-296.

55) T. Hirukawa, Bull. Geol. Survey Japan, 19,(1968) 671-682.

56) S. Maki, J. Japanese Association of Petroleum Technologists, 38, (1973) 28-38,

57) T.Ishikawa, Y. Katsui, Y. Ohba and H. Satoh, On calderas in Hokkaido, Bull. Volcanol. Soc. Japan, 14, (1969) 97-108.

58) Written communication from Japan Metals & Chemicals Co. LTD.

59) E. Mazor, Geothermal tracing with atmospheric and radiogenic noble gases, Geothermics, 5,(1977) 21-36.

60) M. Ozima and E. C. Alexander, Jr., Rare gas fractionation patterns in terrestrial samples and the earth-atmosphere evolution model, Rev. Geophys. Space Phys. 14, (1976) 358-390.

61) K. Nagao, N. Takaoka and O. Matsubayashi, Isotopic anomalies of rare gases in the Nigorikawa geothermal area, Hokkaido, Japan, Earth Planet. Sci. Lett., (in press).

62) K. Rankama, Progress in Isotope Geology, ed. K. Rankama, Interscience Publishers, John Wiley & Sons, New York,London. 1954.

63) M. Tatsumoto, Genetic relations of oceanic basalts as indicated by lead isotopes, Science, 153, (1966) 1094.

64) F. Aumento and R. D. Hyndman, Uranium content of the ocenic upper mantle, Earth Planet. Sci. Lett., 12,(1971) 373-384.

65) J. D. MacDougall, Uranium in marine basalts: concentration, distribution and implications, Earth Planet. Sci. Lett., 35, (1977) 65-70.

66) Geotimes, 22,(No. 6) (1977) 21-23.

67) N. Takaoka and K. Nagao, Rare-gas studies of Cretaceous deep-sea basalts, DSDP Initial Report, Leg 51-53, (in press).

68) D. H. Green, J. W. Morgan and K. S. Heier, Thorium, uranium and ptassium abundances in peridotite inclusions and their hosts, Earth Planet. Sci. Lett., 4, (1968) 155

69) D. J. Kleeman, D. H. Green and J. F. Lovering, Uranium distributions in ultramafic inclusions from Victorian basalts, Earth Planet. Sci. Lett.,5, (1969) 449

70) F. Hoyle and W. A. Fowler, On the abundances of uranium and thorium in solar system material, in Isotopic and Cosmic Chemistry (1964) 516

71) H. Okada, Fine structure of the upper mantle beneath Japanese island arcs as revealed from body wave analyses (1977) Thesis presented to Univ. Hokkaido.

72) H. Craig, W. B. Clarke and M. A. Beg, Excess ^{3}He in deep water on the east Pacific Rise, Earth Planet. Sci. Lett., 26,(1975)125-132

73) H. E. Johnson and W. I. Axford, Production and loss of ^{3}He in the earth's atmosphere, J. Geophys. Res., 74,(1969) 2433-2438.

74) I. N. Tolstikhin, A review: Some recent advances in isotopic geochemistry of light rare gases, in Terrestrial Rare Gases, ed. E. C. Alexander, Jr. and M. Ozima, pp.33-62, Cent. Acad. Publ.Japan, Tokyo, 1978.

75) A. B. Verkhovskii and Yu. A. Shukolyukov, On the possible occurrence of primordial Neon in sudberite of Monchegorsk Pluton, Dokl. Akad. Nauk USSR, 224, (1975) 685-688. (in Russian).

76) G. S. Anufriev, I. L. Kamenskii and V. P. Pavlov, Anomalous isotopic composition of neon in hot-springs of modern volcanic zones, Dokl. Akad. Nauk USSR, 231,(1976) 1454-1457 (in Russian)

77) G. J. F. MacDonald, The escape of helium from the earth's atmosphere, *in* The origin and evolution of atmospheres and oceans, ed. Brancazio and Cameron, John Wiley & Sons, (1964)

78) W. E. Potter and D. C. Kayser, In situ measurments of neon in the thermosphere, Geophys. Res. Lett., 3, (1976) 665-668.

79) G. B. Dalrymple, $^{40}Ar/^{36}Ar$ analyses of histric lava flows, Earth Planet. Sci. Lett., 6, (1969) 47-55

80) D. Krummenacher, Isotopic composition of argon in modern surface volcanic rocks, Earth Planet. Sci. Lett., 8, (1970) 109-117

81) J. Dymond and L. Hogan, Noble gas abundance patterns in deep-sea basalts - Primordial gases from the mantle, Earth Planet. Sci. Lett., 20, (1973) 131-139.

82) F. J. Norton, J. Amer. Ceram. Soc., 36, (1953) 90-96.

83) R. Sugisaki, Changing He/Ar and N_2/Ar ratios of fault air may be earthquake precursors, Nature, 275,(1978) 209-211.

84) see references quoted by Wakita et al. *in* Science 200, (1978) 430-432.

85) G. Kockarts, Space sci. Rev., 14, (1973) 723

86) R. A. Canalas, E. C. Alexander, Jr. and O. K. Manuel, Terrestrial abundance of noble gas, J. Geophys. Res., 73, (1968) 3331-3334.

87) T. Fukutomi, J. Fac. Sci. Hokkaido Univ. Ser. VII, 1, (1960) 223.

Figure captions

Fig. II-1. Sampling localies in the Japanese Islands are shown. Descriptions of samples are summarized in Table II-1.

Fig. II-2a. Collection method of bubble gases. A plastic tube and a sampling vessel are first filled with local water through a funnel with the aid of a manual pump. Then accumulated bubble gas is transfered into the sampling vessel by replacing the water.

Fig. II-2b. Collection method of soil gas samples. A pipe is sealed in a hole and left sealed a day. Accumulated soil gas is transfered into a sampling vessel with the aid of a manual pump. The vessel is flushed several times with the sample gas to remove the atmospheric contamination.

Fig. II-3. Schematic diagram of a line used for rare gas analysis.

Fig. II-4. A trace of He spectrum. The resolving power was adjusted to about 600 to separate ^{3}He from H_3 and HD peaks.

Fig. II-5. Variation of $(^{21}Ne + {}^{20}NeH)/{}^{20}Ne$ ratio is shown. An appearence of ^{20}NeH varied depending on pressure of He and Ne in the ion source. The $^{22}Ne/{}^{20}Ne$ ratio is approximately constant at a wide range of the ion source pressure.

Fig. II-6. Variations of sensitivities of the mass spectrometer for He and Ne are shown. The sensitivities were also affected by the high pressure of He and Ne.

Fig. III-1. Distribution of $^3He/^4He$ ratio in the Japanese Islands. The $^3He/^4He$ ratios relative to the atmospheric ratio defined by Eq. III-1 are shown. Symboles represent the classification of gas samples as used in Fig. II-1. ^3He enrichments, about seven times the atmospheric ratio, are found in many samples.

Fig. III-2. Correlation between $^3He/^4He$ and $^4He/^{20}Ne$ ratios. A mixing line represents a composition of a mixture between the atmosphere and a He-enriched gas with a high $^3He/^4He$ ratio of 1.0×10^{-5}. All data lie on or below the mixing line, except for sample Gl-ON. The $^3He/^4He$ ratios below the mixing line can be interpreted as admixture of radiogenic ^4He.

Fig. III-3. Calculated isotopic composition for three-component mixture. The components are atmospheric, crustal and mantle gases. The calculation is described in Section III-2b.

Fig. III-4. Plot of $^3He/^4He$ ratio against He concentration. Because the acid component was removed for most of volcanic gases, the initial compositions should be represented by the points which were shifted leftward.

Fig. III-5. Correlation between He concentration and chemical composition of gas sample. N_2-rich gas shows high concentration of He, whereas He concentration is low in CO_2-rich gas.

Fig. III-6. Correlation between $^3He/^4He$ ratio and CO_2 concentration for samples collected in the Nigorikawa geothermal area.

Fig. III-7. Correlation diagram of $\delta(22/20)$ and $\delta(38/36)$. The deviation relative to the atmospheric values found in volcanic gas samples cannot be explained by the mass fractionation of atmosphere.

Fig. III-8. Correlation diagram of $\delta(38/36)$ and $\delta(40/36)$. Most of Japanese gas samples show small enrichment in radiogenic ^{40}Ar. The samples with low $^{38}Ar/^{36}Ar$ and $^{40}Ar/^{36}Ar$ ratios are well expressed by the mass fractionation of atmospheric Ar.

Fig. III-9a. Mass fractionated Kr found in samples collected in the Nigorikawa geothermal area.

Fig. III-9b. Mass fractionated Xe found in samples collected in the Nigorikawa geothermal area.

Fig. III-10a ~ Fig. III-10d. Elemental abundance patterns for gas samples. Fractionated abundance pattern for the atmospheric rare gases dissolved in low temperature water is also shown for comparison.

Fig. Ⅳ-1. A model of a tectonic structure under the Japanese Islands.

Table II-1. Sampling localities and classification of samples.

Sample No.		Locality	Prefecture	Date
	Volcanic gas			
1.	V1-TK	Tokachidake	Hokkaido	1974.9.
2.	V2-SS-1	Showa-shinzan	Hokkaido	1958.8.12.
3.	-2			1959.7.9.
4.	-3			1959.7.1.
5.	-4			1964.9.23.
6.	-5			1965.10.6.
7.	-6			1974.9.1.
8.	-7			1977.10.2.
9.	V3-US	Usu	Hokkaido	1978.10.9.
10.	V4-NS	Nasudake	Tochigi	1970.7.24.
11.	V5-HK	Hakone	Kanagawa	1976.7.6.
12.	V6-TT	Tateyama	Toyama	1978.9.30.
13.	V7-KJ	Kuju	Oita	1976.2.6.
14.	V8-KS	Kirishima	Miyazaki	1978.12.30.
15.	V9-SI-1	Satsuma-Iwojima, Kuromoe Shita	Kagoshima	1974.8.12.
16.	-2	Kuromoe Ue		1967.
	Hot-spring gas			
17.	H1-IW	Iwama	Ishikawa	1978.9.27.
18.	H2-SR	Shiramine	Ishikawa	1978.9.28.
19.	H3-YN	Yunomine	Wakayama	1978.4.29.
20.	H4-KW	Kawayu	Wakayama	1978.4.30.
21.	H5-AR	Arima	Hyogo	1978.8.24.
22.	H6-YM	Yumura	Hyogo	1978.8.25.

23.	H7-MS	Misasa	Tottori	1978.8.25.
24.	H8-YB	Yubara	Okayama	1978.8.15.
25.	H9-KI	Kaike	Tottori	1978.11.30.
26.	H10-MT	Matsue	Shimane	1978.11.30.
27.	H11-KY	Koyahara	Shimane	1978.12.1.
28.	H12-YN	Yunotsu	Shimane	1978.12.1.
29.	H13-BP	Beppu	Oita	1978.12.29.
30.	H14-YK	Yamakawa	Kagoshima	1979.1.1.
	Bubble gas in low temperature water pool			
31.	L1-NG	Nigorikawa	Hokkaido	1977.10.
32.	L2-MC	Matsushiro CO_2-rich gas	Nagano	1977.6.13.
33.	L3-YS	Yoshino	Nara	1978.9.24.
34.	L4-NM	Nameri	Osaka	1978.8.23.
35.	L5-IS	Ishibotoke	Osaka	1978.8.23.
36.	L6-KW	Kawanishi	Hyogo	1978.9.6.
37.	L7-IK	Ikeda	Shimane	1978.12.1.
	Soil gas			
38.	S1-NG-1	Nigorikawa A15	Hokkaido	1977.10.
39.	-2	A23		
40.	-3	A29		
41.	-4	A31		
42.	-5	E26		
43.	S2-MN	Matsushiro N_2-rich gas	Nagano	1977.6.13.
44.	S3-SZ	Shuzenzi	Shizuoka	———
	Geothermal prospecting well gas			
45.	G1-ON	Onuma	Akita	1976.10.
46.	G2-TK	Takenoyu	Oita	1977.3.13.

Well gas for earthquake prediction

47.	W1-MT	Mitsubishi	Kanagawa	1977.1.
48.	W2-KW	Kawasaki	Kanagawa	1977.2.10.

Continental CO_2 well gas, Derbecen, Hungary

49.	DR-05	Derbecen #5		1978.
50.	DR-63	#63		1978.
51.	DR-65	#65		1978.

Solid sample

52.	RB-56	Atlantic Ridge basalt	#56	1966.
53.	RB-197		#197	1968.
54.	VL-IO	Volcanic lava, Izu-Oshima		
55.	VL-NS		Nishinoshima-shinto	1975.8.25.
56.	VL-HY		Hiyoshioki-no-ba	1977.5.29.

Table II-2. Chemical compositions of gas samples.

Hot-spring gases and other types of bubble gases.

composition	H3-YN	H4-KW	H5-AR	H6-YM	H11-KW	H12-YN	L3-YS	L4-NM	L5-IS	L6-KW	L7-IK
vol. %	[53]*	[53]*	[53]*	[54]*	[55]*	[55]*	[53]*	[53]*	[53]*	[54]*	[55]*
He	>0.0005 <0.001	0.015	>0.0005 <0.001	0.037	tr	0.004	0.000	0.003	0.000	0.000	0.000
H_2	0.068	0.008	0.831	0.111	0.001	0.020	0.000	0.000	0.000	0.000	tr
O_2	0.41	0.20	0.38	0.69	2.04	0.27	0.82	0.40	0.13	5.29	0.14
N_2	3.24	57.51	1.18	77.22	1.15	10.37	3.60	4.60	0.82	22.68	0.64
CH_4	3.38	31.71	0.03	0.69	tr	0.20	0.14	6.80	1.16	0.76	tr
CO_2	92.91	10.57	97.58	21.26	96.81	88.99	95.44	88.20	97.89	71.27	99.21

* references

Table II-2. Chemical compositions of gas samples.

Volcanic gases. (quoted by [38])

Chemical composition	Showa-shinzan		Nasudake	Satsuma-Iwojima
(ml/l)	A - 1 #	C - 2 #		
H_2	0.83	1.21	o.17	0.72
CO_2	0.32	3.66	1.12	4.7
N_2	} 0.079	0.21	0.19	0.04
CH_4		8×10^{-3}	32×10^{-3}	8×10^{-6}
SO_2	0.080	0.091	0.26	8.2
H_2S	0.008	0.030	1.22	0.5
O_2	0.018	——	——	——
HCl	0.035	——	0.25	4.9
HF	0.14	——	——	0.40
H_2O	998.2	994.1	996.8	981

fumaroles

Table III-1a. Isotopic compositions of He, Ne and Ar.

Sample No.	$^{3}He/^{4}He$ (x 10^{-6})	$^{21}Ne/^{20}Ne$	$^{22}Ne/^{20}Ne$	$^{38}Ar/^{36}Ar$	$^{40}Ar/^{36}Ar$
1. V1-TK	9.19 ± 0.55	0.00292 ± 0.00006	0.1007 ± 0.0008	0.187 ± 0.001	305 ± 2
2. V2-SS-1	7.41 ± 0.31	0.00296 ± 0.00005	0.1016 ± 0.0005	0.186 ± 0.001	302.5 ± 1.2
3. V2-SS-2	6.67 ± 0.40				
4. V2-SS-3	7.00 ± 0.19	0.00301 ± 0.00006	0.1001 ± 0.0004		
5. V2-SS-4	7.04 ± 0.53	0.00291 ± 0.00013	0.1006 ± 0.0012	0.188 ± 0.003	303 ± 2
6. V2-SS-5	7.01 ± 0.53	0.00296 ± 0.00009	0.1014 ± 0.0005		
7. V2-SS-6	3.91 ± 0.24	0.00282 ± 0.00002	0.0966 ± 0.0003	0.185 ± 0.002	286.6 ± 1.6
8. V2-SS-7	3.13 ± 0.32	0.00295 ± 0.00007	0.0980 ± 0.0003		
9. V3-US	9.62 ± 0.42	0.00294 ± 0.00008	0.0983 ± 0.0008	0.187 ± 0.001	312.9 ± 1.1
10. V4-NS	6.66 ± 0.29	0.00295 ± 0.00004	0.1005 ± 0.0007	0.188 ± 0.001	304.7 ± 1.5
11. V5-HK	8.51 ± 0.40	0.00301 ± 0.00009	0.1017 ± 0.0014	0.188 ± 0.002	297.7 ± 0.9
12. V6-TT	10.9 ± 0.8	0.00293 ± 0.00004	0.1022 ± 0.0006	0.186 ± 0.001	299.3 ± 1.7
13. V7-KJ	10.5 ± 0.3	0.00283 ± 0.00009	0.0978 ± 0.0007	0.184 ± 0.001	294.9 ± 0.7
14. V8-KS	10.3 ± 0.7	0.00292 ± 0.00004	0.1016 ± 0.0006		
15. V9-SI-1	10.2 ± 0.6	0.00285 ± 0.00005	0.0995 ± 0.0006	0.186 ± 0.001	289.9 ± 0.7
16. V9-SI-2	10.6 ± 0.5				
17. H1-IW	11.4 ± 1.1	0.00285 ± 0.00005	0.1011 ± 0.0004	0.187 ± 0.002	291.5 ± 2.1
18. H2-SR	5.65 ± 0.27	0.00299 ± 0.00008	0.1025 ± 0.0006	0.187 ± 0.001	325.1 ± 1.2

Table III-1a. Isotopic compositions of He, Ne and Ar.

Sample No.	$^{3}He/^{4}He$ ($\times 10^{-6}$)	$^{21}Ne/^{20}Ne$	$^{22}Ne/^{20}Ne$	$^{38}Ar/^{36}Ar$	$^{40}Ar/^{36}Ar$
19. H3-YM	6.56 ± 0.28		0.1026 ± 0.0008		
20. H4-KW	5.65 ± 0.37				
21. H5-AR	11.0 ± 0.4	0.00308 ± 0.00006	0.1018 ± 0.0007	0.188 ± 0.002	303.3 ± 1.0
22. H6-YM	7.50 ± 0.18	0.00293 ± 0.00009	0.1013 ± 0.0006	0.185 ± 0.002	297.6 ± 1.7
23. H7-MS	8.35 ± 0.30		0.1022 ± 0.0007	0.187 ± 0.002	301.7 ± 2.1
24. H8-YB	3.96 ± 0.22		0.1022 ± 0.0006		
25. H9-KI	7.66 ± 0.11	0.00296 ± 0.00005	0.1020 ± 0.0006	0.187 ± 0.002	304.9 ± 1.5
26. H10-MT	5.94 ± 0.28	0.00298 ± 0.00005	0.1015 ± 0.0007	0.188 ± 0.002	300.3 ± 1.6
27. H11-KY	9.15 ± 0.52	0.00290 ± 0.00004	0.1021 ± 0.0006	0.187 ± 0.002	309.1 ± 1.5
28. H12-YN	9.12 ± 0.57	0.00301 ± 0.00004	0.1028 ± 0.0006	0.187 ± 0.002	315.1 ± 2.0
29. H13-BP	9.00 ± 0.47	0.00297 ± 0.00004	0.1018 ± 0.0005		
30. H14-YK	9.84 ± 0.56	0.00292 ± 0.00004	0.1016 ± 0.0005		
31. L1-NG	9.95 ± 0.25	0.00299 ± 0.00009	0.1005 ± 0.0008	0.185 ± 0.002	325 ± 7
32. L2-MC	9.10 ± 0.69	0.00292 ± 0.00007	0.1016 ± 0.0012	0.186 ± 0.004	304 ± 8
33. L3-YS	6.44 ± 0.80	0.00293 ± 0.00003	0.1001 ± 0.0005	0.187 ± 0.001	296.4 ± 1.1
34. L4-NM	10.4 ± 0.3	0.00311 ± 0.00006	0.1016 ± 0.0009	0.187 ± 0.002	315.9 ± 1.4
35. L5-IS	6.45 ± 0.48	0.00303 ± 0.00005	0.1025 ± 0.0008	0.186 ± 0.001	295.9 ± 0.9
36. L6-KW	1.53 ± 0.06	0.00296 ± 0.00005	0.1021 ± 0.0010	0.189 ± 0.002	306.1 ± 1.2

Table III-1a. Isotopic compositions of He, Ne and Ar.

Sample No.	$^{3}He/^{4}He$ ($\times 10^{-6}$)	$^{21}Ne/^{20}Ne$	$^{22}Ne/^{20}Ne$	$^{38}Ar/^{36}Ar$	$^{40}Ar/^{36}Ar$
37. L7-IK	8.58 ± 0.44	0.00292 ± 0.00006	0.1018 ± 0.0007	0.188 ± 0.002	309.9 ± 1.6
38. S1-NG-1	3.00 ± 0.15	0.00290 ± 0.00004	0.0972 ± 0.0006	0.180 ± 0.002	276 ± 2
39. S1-NG-2	2.16 ± 0.25	0.00292 ± 0.00005	0.1009 ± 0.0006	0.184 ± 0.002	293 ± 2
40. S1-NG-3	4.55 ± 0.27	0.00279 ± 0.00006	0.1001 ± 0.0009	0.183 ± 0.002	283 ± 6
41. S1-NG-4	4.38 ± 0.29	0.00286 ± 0.00006	0.0968 ± 0.0009	0.179 ± 0.002	276 ± 7
42. S1-NG-5	1.60 ± 0.07	0.00319 ± 0.00006	0.1012 ± 0.0007	0.186 ± 0.002	292 ± 2
43. S2-MN	9.12 ± 0.58	0.00292 ± 0.00010	0.1011 ± 0.0009	0.187 ± 0.003	308 ± 9
44. S3-SZ	1.67 ± 0.17				
45. G1-ON	15.4 ± 0.4	0.00297 ± 0.00005	0.1017 ± 0.0005	0.189 ± 0.002	300.1 ± 1.8
46. G2-TK	5.70 ± 0.40				
47. W1-MT	$<$0.3	0.00298 ± 0.00004	0.1020 ± 0.0004		
48. W2-KW	0.86 ± 0.32		0.1017 ± 0.0004		
49. DR-05	0.62 ± 0.07			0.187 ± 0.002	364.7 ± 2.3
50. DR-63	0.42 ± 0.03			0.187 ± 0.002	844.8 ± 3.8
51. DR-65	0.46 ± 0.05			0.187 ± 0.002	607.0 ± 3.7

Table III-1a. Isotopic compositions of He, Ne and Ar.

Sample No.	$^{3}He/^{4}He$ ($\times 10^{-6}$)	$^{21}Ne/^{20}Ne$	$^{22}Ne/^{20}Ne$	$^{38}Ar/^{36}Ar$	$^{40}Ar/^{36}Ar$
52. RB-56	9.88 ± 0.57	0.00312 ± 0.00014	0.1012 ± 0.0009	0.188 ± 0.002	328 ± 2
53. RB-197	10.1 ± 0.5	0.00319 ± 0.00013	0.1010 ± 0.0015	0.190 ± 0.003	451 ± 6
54. VL-IO		0.00299 ± 0.00016	0.1042 ± 0.0007	0.183 ± 0.003	285 ± 5
55. VL-NS					
800°C		0.00284 ± 0.00010	0.1007 ± 0.0007	0.182 ± 0.002	285 ± 2
1800°C		0.00334 ± 0.00012	0.1076 ± 0.0010	0.181 ± 0.008	271 ± 12
56. VL-HY					
800°C		0.00279 ± 0.00008	0.0988 ± 0.0006	0.185 ± 0.002	294 ± 3
1800°C		0.00279 ± 0.00008	0.1003 ± 0.0009	0.183 ± 0.002	284 ± 2

Table III-1b. Elemental compositions and concentrations.

Sample No.	^{4}He(ppm)	^{36}Ar(ppm)	$^{4}He/^{36}Ar$	$^{20}Ne/^{36}Ar$	$^{84}Kr/^{36}Ar$	$^{132}Xe/^{36}Ar$	$^{4}He/^{20}Ne$
1. V1-TK			9.7	0.28	0.052		35
2. V2-SS-1	28	0.58	48	0.39	0.060	0.0057	120
3. V2-SS-2	23						2.1
4. V2-SS-3	130						10
5. V2-SS-4			15	0.20	0.035	0.0027	75
6. V2-SS-5	5.1						86
7. V2-SS-6	4.7						2.0
8. V2-SS-7	0.82						0.61
9. V3-US	11	0.083	130	0.20	0.064	0.0079	650
10. V4-NS	17	0.44	40	0.41	0.046	0.0028	97
11. V5-HK	42	6.2	6.7	0.30	0.048	0.0034	23
12. V6-TT	5.1	0.41	12	0.57	0.034	0.0016	22
13. V7-KJ	210	8.5	25	0.39	0.039	0.0016	64
14. V8-KS	16						24
15. V9-SI-1	14	4.6	3.0	0.31	0.043	0.0033	9.6
16. V9-SI-2							16
17. H1-IW	0.93	0.66	1.4	0.18	0.053	0.0063	8.1
18. H2-SR	1200	8.3	150	0.32	0.031	0.00078	470

Table III-1b. Elemental compositions and concentrations.

Sample No.	^{4}He(ppm)	^{36}Ar(ppm)	$^{4}He/^{36}Ar$	$^{20}Ne/^{36}Ar$	$^{84}Kr/^{36}Ar$	$^{132}Xe/^{36}Ar$	$^{4}He/^{20}Ne$
19. H3-YN	58						63
20. H4-KW	12						1.0
21. H5-AR	14	0.44	32	0.16	0.059	0.0044	210
22. H6-YM	300	33	9.3	0.15	0.052	0.0033	62
23. H7-MS	940	20	48	0.31	0.046	0.0030	150
24. H8-YB	54						10
25. H9-KI	1300	32	40	0.22	0.045	0.0024	180
26. H10-MT	1800	38	48	0.25	0.045	0.0025	200
27. H11-KY	5.3	0.53	9.9	0.065	0.078	0.0064	160
28. H12-YN	40	2.7	15	0.13	0.057	0.0039	120
29. H13-BP	31						75
30. H14-YK	29						7.0
31. L1-NG	4.0	0.058	69	0.25	0.038	0.0032	280
32. L2-MC	5.0	1.0	4.9	0.24	0.053	0.0049	20
33. L3-YS	1.0	0.22	4.6	0.37	0.059	0.0036	12
34. L4-NM	45	0.32	140	0.18	0.043	0.0024	780
35. L5-TS	0.60	0.073	8.2	0.28	0.070	0.0063	30
36. L6-KW	110	4.1	26	0.23	0.043	0.0025	110

Table III-1b. Elemental compositions and concentrations.

Sample No.	^{4}He(ppm)	^{36}Ar(ppm)	$^{4}He/^{36}Ar$	$^{20}Ne/^{36}Ar$	$^{84}Kr/^{36}Ar$	$^{132}Xe/^{36}Ar$	$^{4}He/^{20}Ne$
37. L7-IK	11	0.63	17	0.095	0.076	0.0053	180
38. S1-NG-1	4.9	3.6	1.4	1.4	0.0095	0.00016	1.0
39. S1-NG-2	5.4	20	0.27	0.58	0.023	0.00058	0.45
40. S1-NG-3	4.0	8.7	0.46	0.61	0.018	0.00094	0.75
41. S1-NG-4	4.0	2.6	1.5	1.6	0.0085	0.000087	0.95
42. S1-NG-5	4.7	21	0.23	0.52	0.021	0.0062	0.43
43. S2-MN	300	7.2	48	0.27	0.031	0.0017	180
44. S3-SZ	4.8						0.27
45. G1-ON	5.3	3.5	1.5	0.65	0.028	0.0013	2.3
46. G2-TK							0.75
47. W1-MT	39						23
48. W2-KW	1.4						0.72
49. DR-05	140	0.36	400	0.17	0.034	0.0024	2300
50. DR-63	250	0.22	1200	0.14	0.026	0.0054	8100
51. DR-65	300	0.37	800	0.18	0.037	0.0033	4400

Table III-1c. Isotopic compositions of Kr and Xe.

	7. V2-SS-6	9. V3-US	11. V5-HK	32. L2-MC	38. S1-NG-1
^{78}Kr	0.636 ± 0.009	0.631 ± 0.010	0.613 ± 0.019	0.618 ± 0.011	0.636 ± 0.006
^{80}Kr	4.06 ± 0.04	4.02 ± 0.04	3.96 ± 0.06	3.99 ± 0.06	4.06 ± 0.03
^{82}Kr	20.5 ± 0.1	20.5 ± 0.2	20.5 ± 0.2	20.4 ± 0.2	20.5 ± 0.1
^{83}Kr	20.4 ± 0.1	20.4 ± 0.2	20.3 ± 0.2	20.3 ± 0.3	20.4 ± 0.1
^{84}Kr	= 100	= 100	= 100	= 100	= 100
^{86}Kr	30.2 ± 0.3	30.5 ± 0.1	30.5 ± 0.3	30.6 ± 0.2	30.2 ± 0.2
^{124}Xe	0.351 ± 0.011	0.371 ± 0.011	0.366 ± 0.018	0.352 ± 0.028	0.371 ± 0.011
^{126}Xe	0.326 ± 0.008	0.346 ± 0.013	0.331 ± 0.007	0.325 ± 0.015	0.333 ± 0.011
^{128}Xe	7.13 ± 0.06	7.21 ± 0.08	7.21 ± 0.12	7.11 ± 0.16	7.24 ± 0.11
^{129}Xe	98.1 ± 0.9	99.1 ± 0.7	98.7 ± 0.6	98.2 ± 0.2	99.7 ± 1.1
^{130}Xe	15.2 ± 0.2	15.3 ± 0.1	15.3 ± 0.14	15.2 ± 0.3	15.3 ± 0.2
^{131}Xe	79.1 ± 0.6	78.7 ± 0.5	79.1 ± 0.4	78.8 ± 0.5	79.1 ± 0.4
^{132}Xe	= 100	= 100	= 100	= 100	= 100
^{134}Xe	39.0 ± 0.4	38.5 ± 0.2	38.7 ± 0.3	38.7 ± 0.6	38.5 ± 0.4
^{136}Xe	33.2 ± 0.5	32.6 ± 0.4	32.8 ± 0.3	32.9 ± 0.6	32.5 ± 0.3

Table III-1c. Isotopic compositions of Kr and Xe.

	41. S1-NG-4	43. S2-MN	49. DR-05	50. DR-63	51. DR-65
^{78}Kr	0.633 ± 0.009	0.616 ± 0.019	0.634 ± 0.019	0.627 ± 0.007	0.622 ± 0.007
^{80}Kr	4.05 ± 0.03	4.00 ± 0.06	4.01 ± 0.06	4.01 ± 0.03	3.99 ± 0.03
^{82}Kr	20.6 ± 0.1	20.6 ± 0.1	20.4 ± 0.2	20.4 ± 0.1	20.2 ± 0.1
^{83}Kr	20.4 ± 0.1	20.3 ± 0.1	20.3 ± 0.1	20.3 ± 0.1	20.2 ± 0.1
^{84}Kr	= 100	= 100	= 100	= 100	= 100
^{86}Kr	30.2 ± 0.3	30.5 ± 0.3	30.5 ± 0.4	30.3 ± 0.2	30.4 ± 0.1
^{124}Xe	0.372 ± 0.012	0.357 ± 0.021	0.374 ± 0.021	0.360 ± 0.013	0.355 ± 0.012
^{126}Xe	0.340 ± 0.008	0.333 ± 0.011	0.334 ± 0.018	0.334 ± 0.005	0.328 ± 0.009
^{128}Xe	7.23 ± 0.05	7.16 ± 0.15	7.19 ± 0.16	7.14 ± 0.06	7.04 ± 0.14
^{129}Xe	99.4 ± 0.9	98.7 ± 1.3	98.6 ± 1.4	98.8 ± 1.1	97.5 ± 1.7
^{130}Xe	15.3 ± 0.2	15.2 ± 0.2	15.2 ± 0.2	15.2 ± 0.1	15.1 ± 0.2
^{131}Xe	79.2 ± 0.6	79.1 ± 0.5	78.7 ± 0.8	79.2 ± 0.5	78.5 ± 0.7
^{132}Xe	= 100	= 100	= 100	= 100	= 100
^{134}Xe	38.6 ± 0.3	38.7 ± 0.5	38.9 ± 0.4	38.8 ± 0.4	38.9 ± 0.4
^{136}Xe	32.7 ± 0.3	32.9 ± 0.5	33.2 ± 0.4	32.8 ± 0.6	33.4 ± 0.6

Table III-1c. Isotopic compositions of Kr and Xe.

	52. RB-56	53. RB-197	54. VL-IO	55. VL-NS 800°C fraction	1800°C fraction
^{78}Kr	0.628 ± 0.038			0.547 ± 0.030	0.628 ± 0.041
^{80}Kr	4.03 ± 0.10	4.11 ± 0.18	4.19 ± 0.19	4.05 ± 0.12	4.07 ± 0.16
^{82}Kr	20.3 ± 0.4	20.4 ± 0.3	20.5 ± 0.4	20.4 ± 0.4	19.9 ± 0.8
^{83}Kr	20.4 ± 0.4	20.2 ± 0.2	20.2 ± 0.5	20.3 ± 0.3	19.8 ± 0.2
^{84}Kr	= 100	= 100	= 100	= 100	= 100
^{86}Kr	30.5 ± 0.3	30.1 ± 0.5	30.4 ± 1.0	30.2 ± 0.5	30.3 ± 1.0
^{128}Xe	7.17 ± 0.36	7.61 ± 0.68	7.52 ± 0.38	7.44 ± 0.55	6.87 ± 0.61
^{129}Xe	98.0 ± 1.7	100.1 ± 2.3	102.3 ± 1.9	101.8 ± 3.0	98.4 ± 4.2
^{130}Xe	15.1 ± 0.6	15.8 ± 0.7	16.3 ± 0.8	14.5 ± 0.7	14.6 ± 0.6
^{131}Xe	78.9 ± 2.2	80.5 ± 2.7	81.2 ± 3.3	78.7 ± 2.5	78.6 ± 2.8
^{132}Xe	= 100	= 100	= 100	= 100	= 100
^{134}Xe	37.9 ± 1.0	38.8 ± 1.8	38.3 ± 0.5	39.1 ± 1.4	37.4 ± 0.8
^{136}Xe	32.1 ± 1.2	32.1 ± 1.0	31.8 ± 1.2	33.6 ± 1.0	32.6 ± 1.3

Table III-1c. Isotopic compositions of Kr and Xe.

	56. VL-HY 800°C fraction	1800°C fraction
^{78}Kr	0.579 ± 0.044	0.601 ± 0.063
^{80}Kr	3.96 ± 0.14	4.04 ± 0.17
^{82}Kr	20.1 ± 0.4	20.3 ± 0.5
^{83}Kr	20.3 ± 0.5	20.2 ± 0.4
^{84}Kr	= 100	= 100
^{86}Kr	30.6 ± 0.6	30.0 ± 0.8
^{128}Xe	6.97 ± 0.50	
^{129}Xe	98.9 ± 2.6	
^{130}Xe	15.0 ± 0.7	
^{131}Xe	79.9 ± 2.1	
^{132}Xe	= 100	
^{134}Xe	38.5 ± 0.9	
^{136}Xe	31.9 ± 1.5	

Table IV-1. Mass fractionation per fractional mass difference.

Element: X	K(X)*		
	S1-NG-1	S1-NG-4	Mean
Ne	0.53	0.57	0.55
Ar	0.69	0.79	0.74
Kr	0.39	0.35	0.37
Xe	0.43	0.40	0.42

* in unit of % per 1 % mass difference.

Table IV-2. $^{3}He/^{4}He$ and $^{4}He/^{20}Ne$ ratios in samples Showa-shinzan and Usu volcanoes.

	Showa-shinzan							Usu
Sample No.	V2-SS-1	V2-SS-2	V2-SS-3	V2-SS-4	V2-SS-5	V2-SS-6	V2-SS-7	V3-US
year	1958	1959	1959	1964	1965	1974	1977	1978
fumarole	A1	C2	C3	A1	A1	A1	A1	
glass	SB	SB	SB	SB	Pyrex	Pyrex	SB	Pyrex
$(^{3}He/^{4}He)^{*}_{o}$	7.4	6.7	7.0	7.0	7.0	3.9	3.1	9.6
$(^{3}He/^{4}He)^{*}_{c}$	7.6	6.7	7.1		(14)	(4.7)	3.1	
$(^{4}He/^{20}Ne)_{o}$	120	2.1	10	75	86	2.0	0.61	650
$(^{4}He/^{20}Ne)_{c}$	130	2.2	11		84	2.0	0.61	

* unit in 10^{-6}.

Subscripts "o" and "c" mean observed and corrected for permeation of He, respectively.

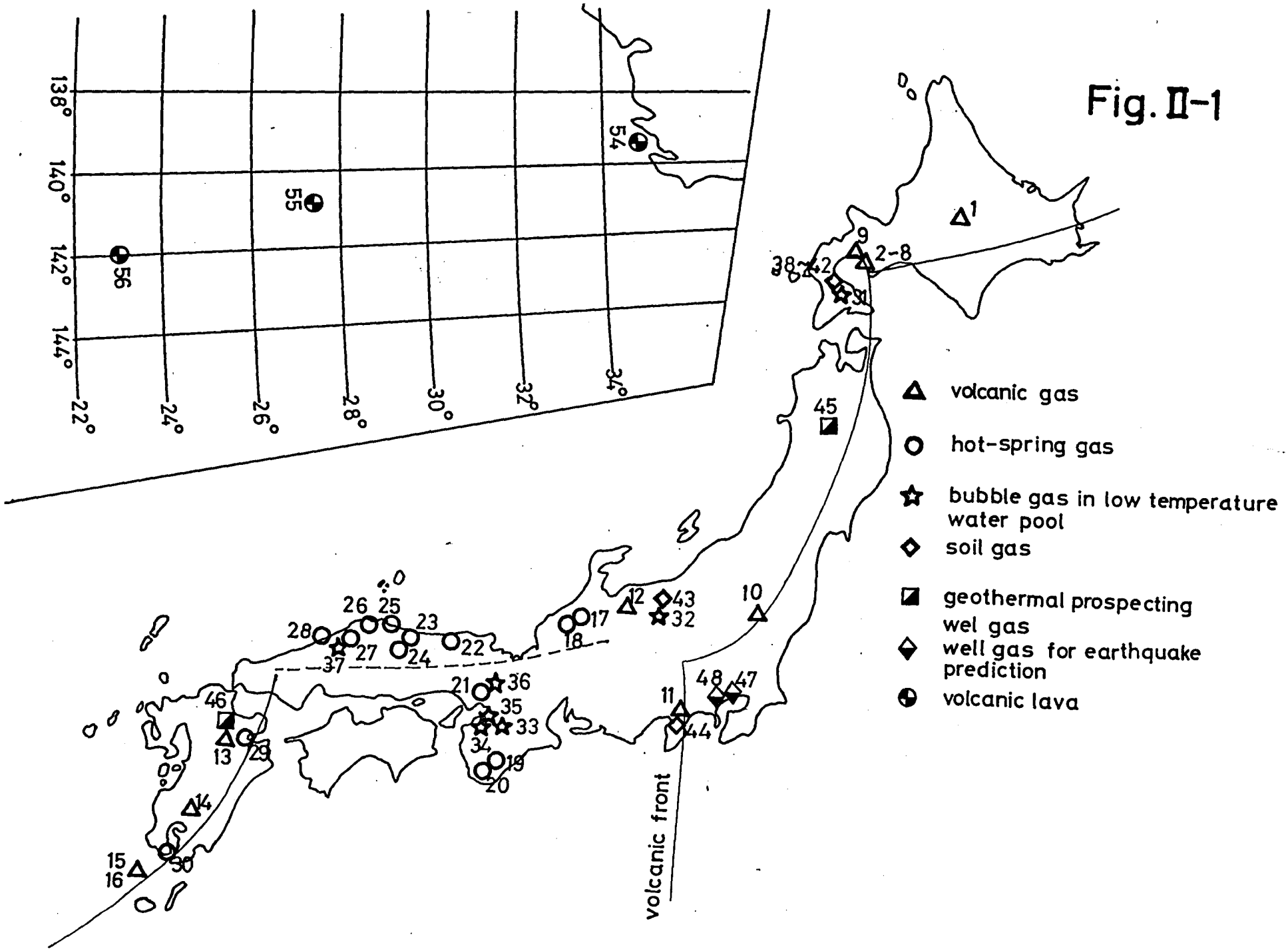
Fig. II-1
volcanic gas
hot-spring gas
bubble gas in low temperature water pool
soil gas
geothermal prospecting wel gas
well gas for earthquake prediction
volcanic lava
volcanic front
138°
140°
142°
144°
22°
24°
26°
28°
30°
32°
34°

Fig. II–2a

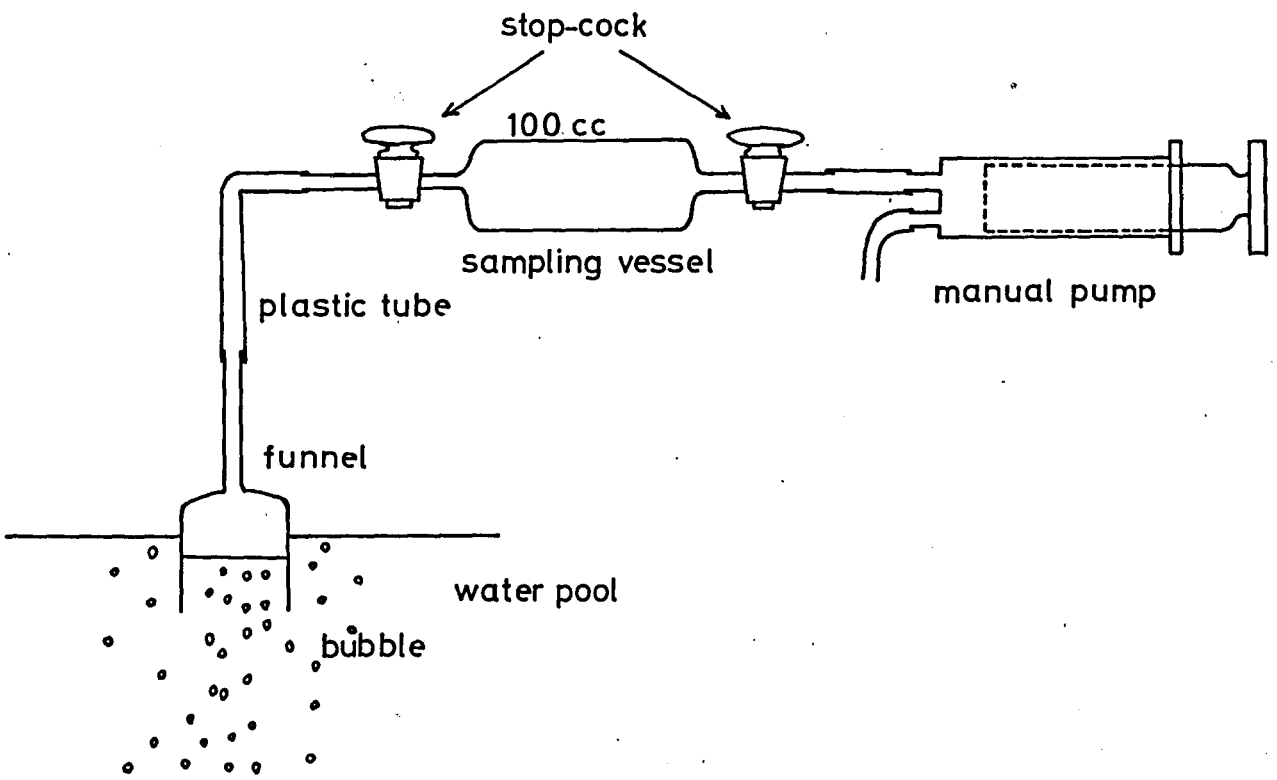
stop-cock
100 cc
sampling vessel
manual pump
plastic tube
funnel
water pool
bubble

Fig.II-2b

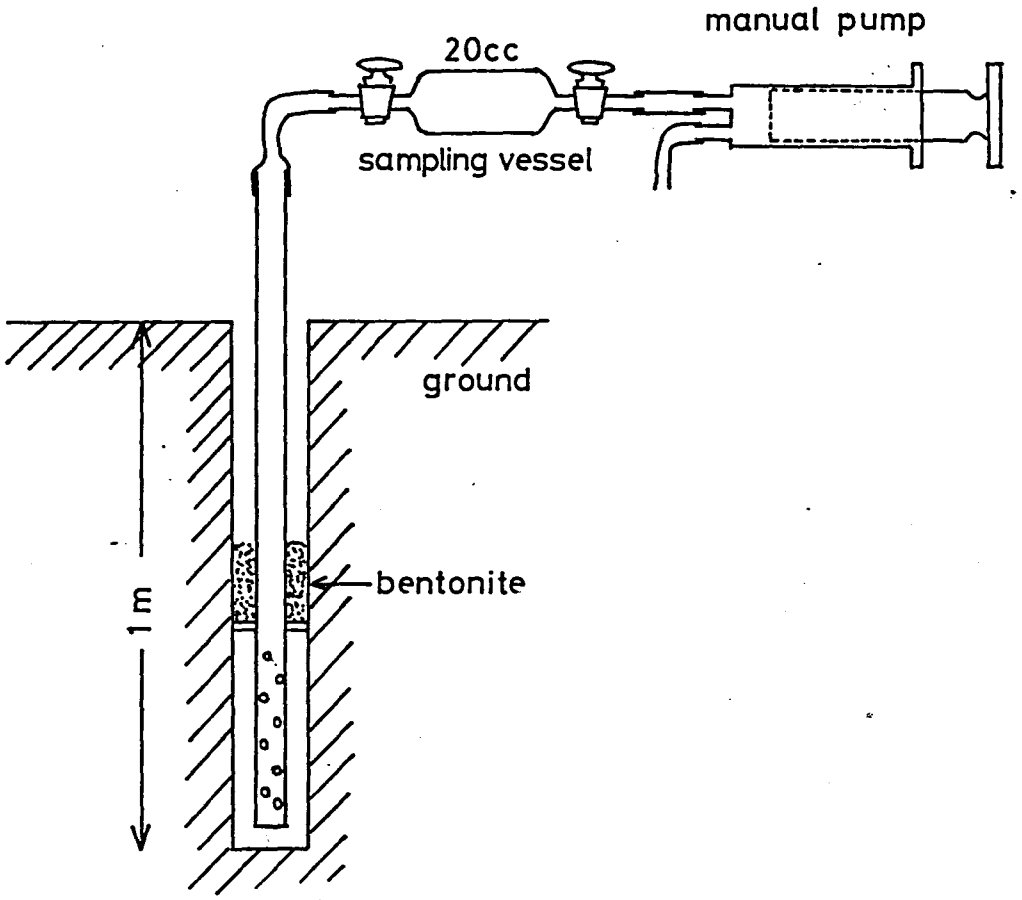

Fig. II-3

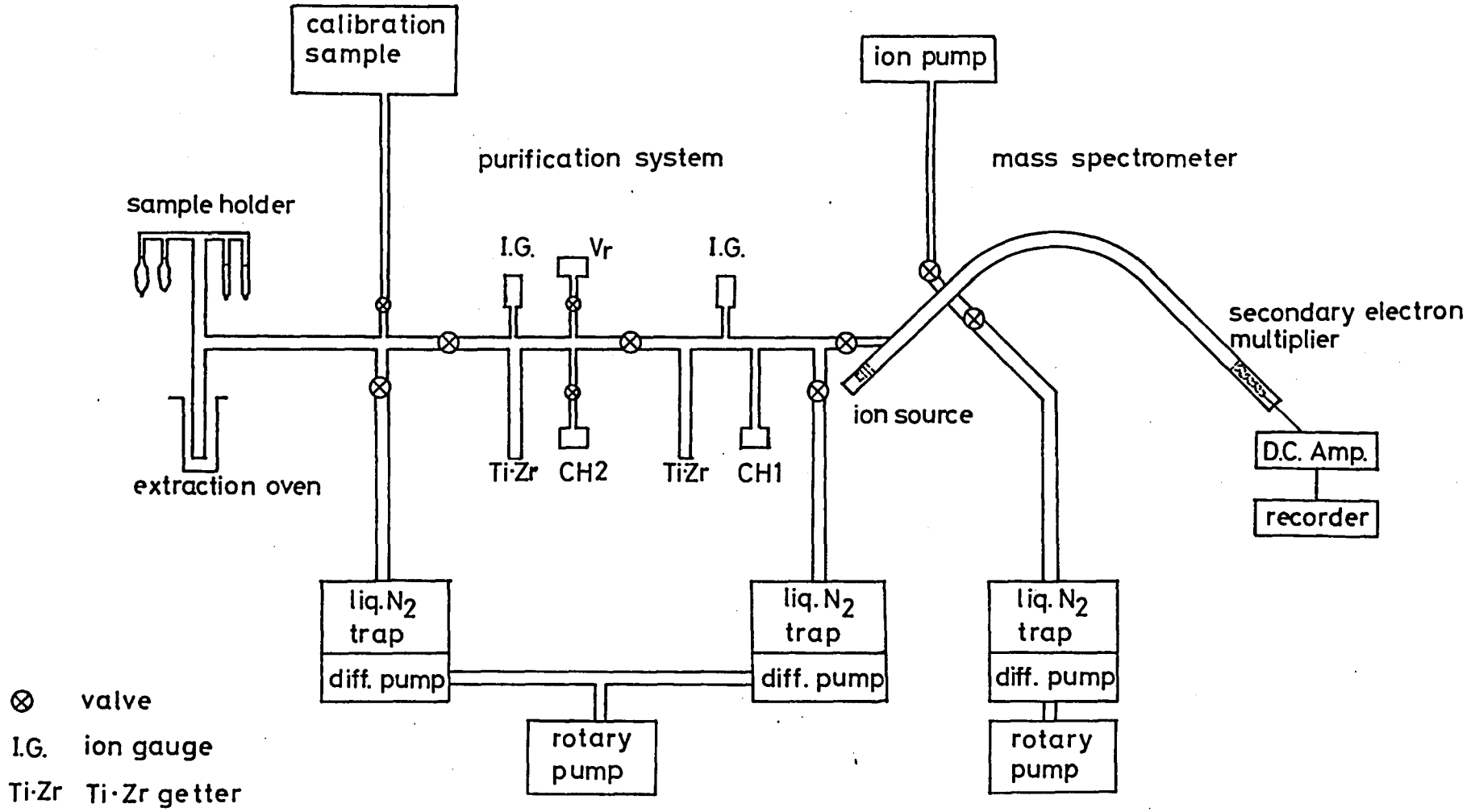
calibration sample
ion pump
purification system
mass spectrometer
sample holder
I.G.
Vr
I.G.
secondary electron multiplier
ion source
D.C. Amp.
recorder
extraction oven
Ti·Zr
CH2
Ti·Zr
CH1
liq. N2 trap
diff. pump
liq. N2 trap
diff. pump
liq. N2 trap
diff. pump
rotary pump
rotary pump
⊗ valve
I.G. ion gauge
Ti·Zr Ti·Zr getter
CH charcoal trap

Fig. II-4

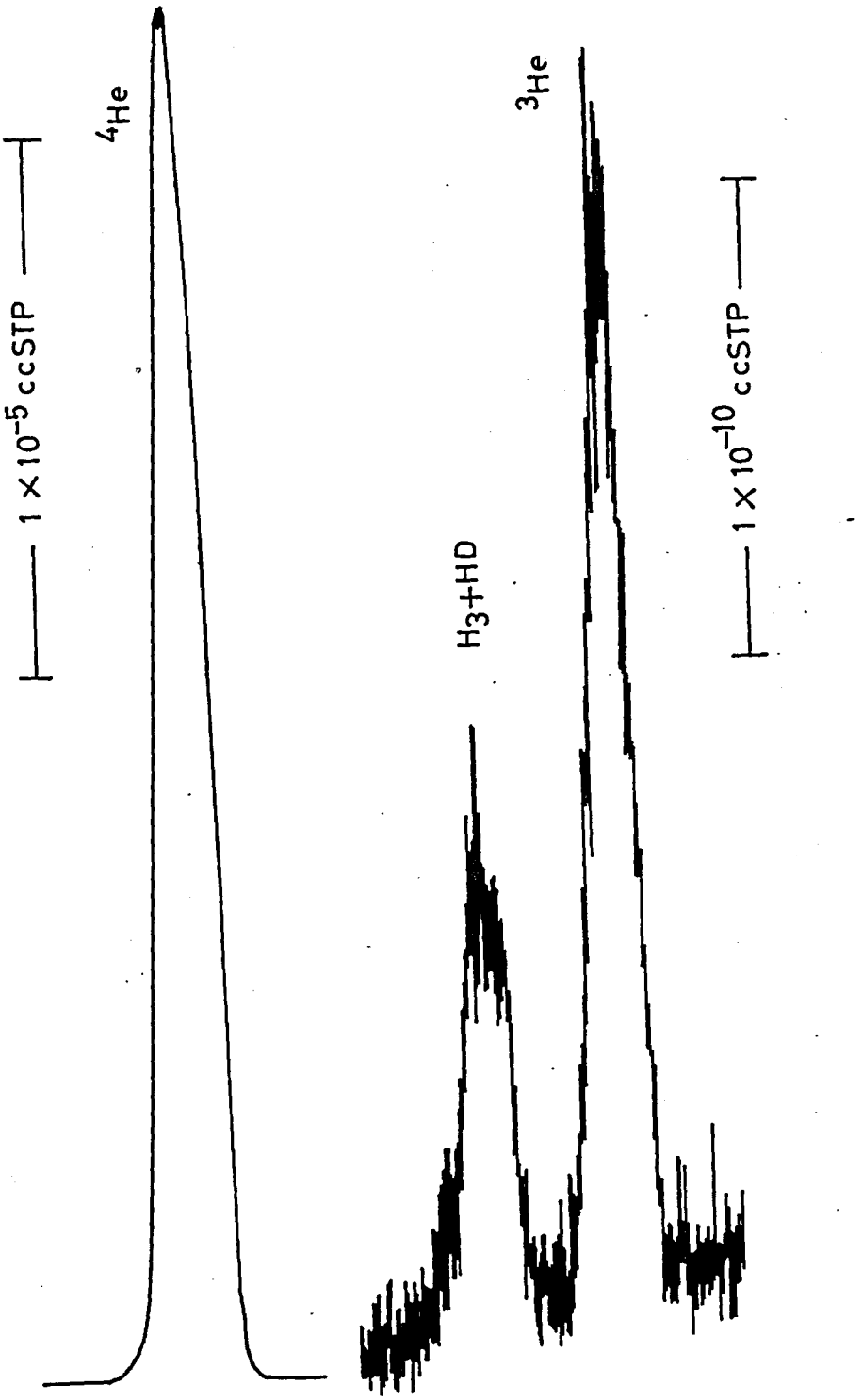

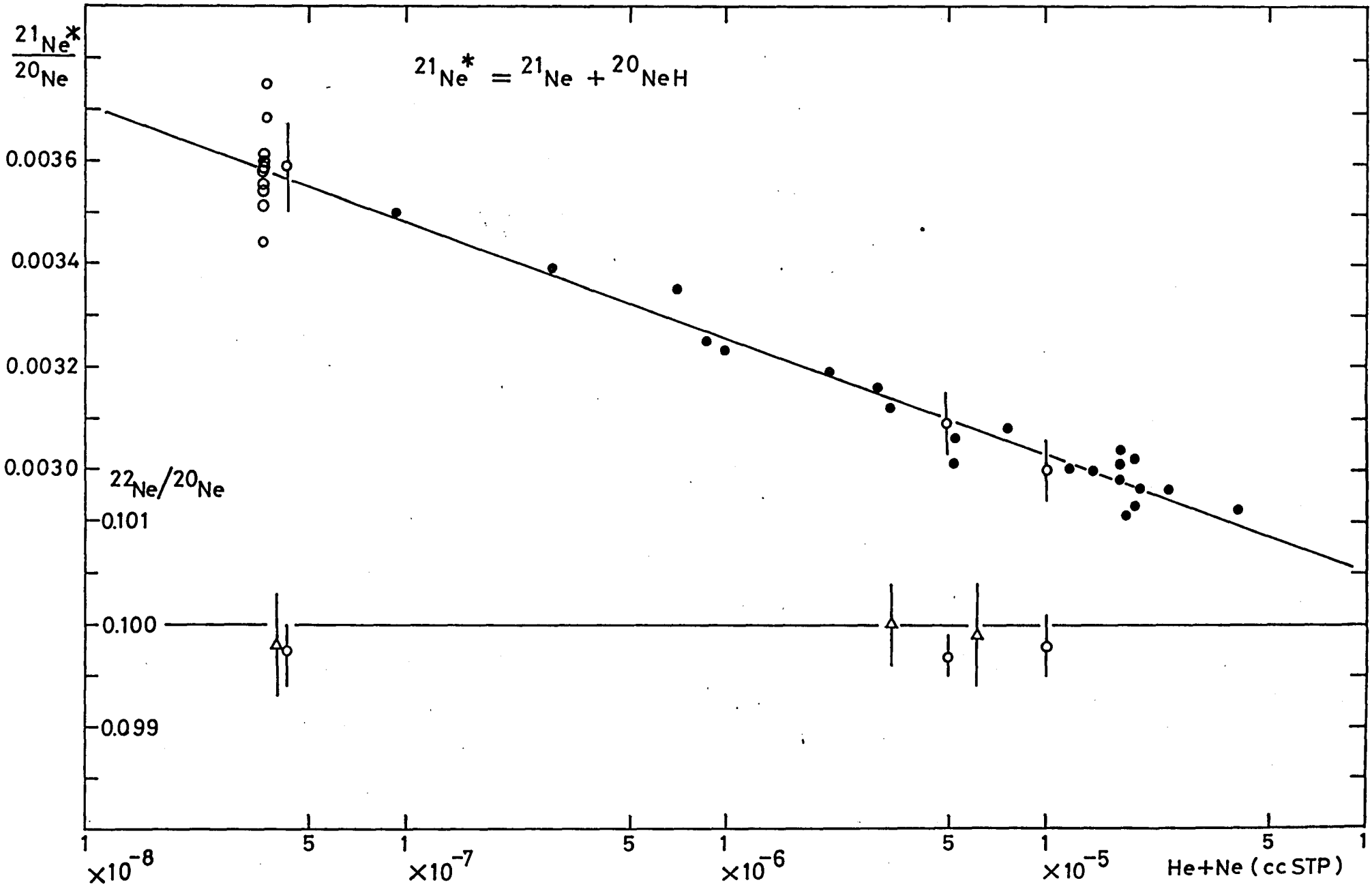
$\frac{21Ne^*}{20Ne}$
$^{21}Ne^* = {}^{21}Ne + {}^{20}NeH$
0.0036
0.0034
0.0032
0.0030
$^{22}Ne/^{20}Ne$
0.101
0.100
0.099
1
5
1
5
1
5
1
5
1
$\times 10^{-8}$
$\times 10^{-7}$
$\times 10^{-6}$
$\times 10^{-5}$
He+Ne (cc STP)

Fig. II-6

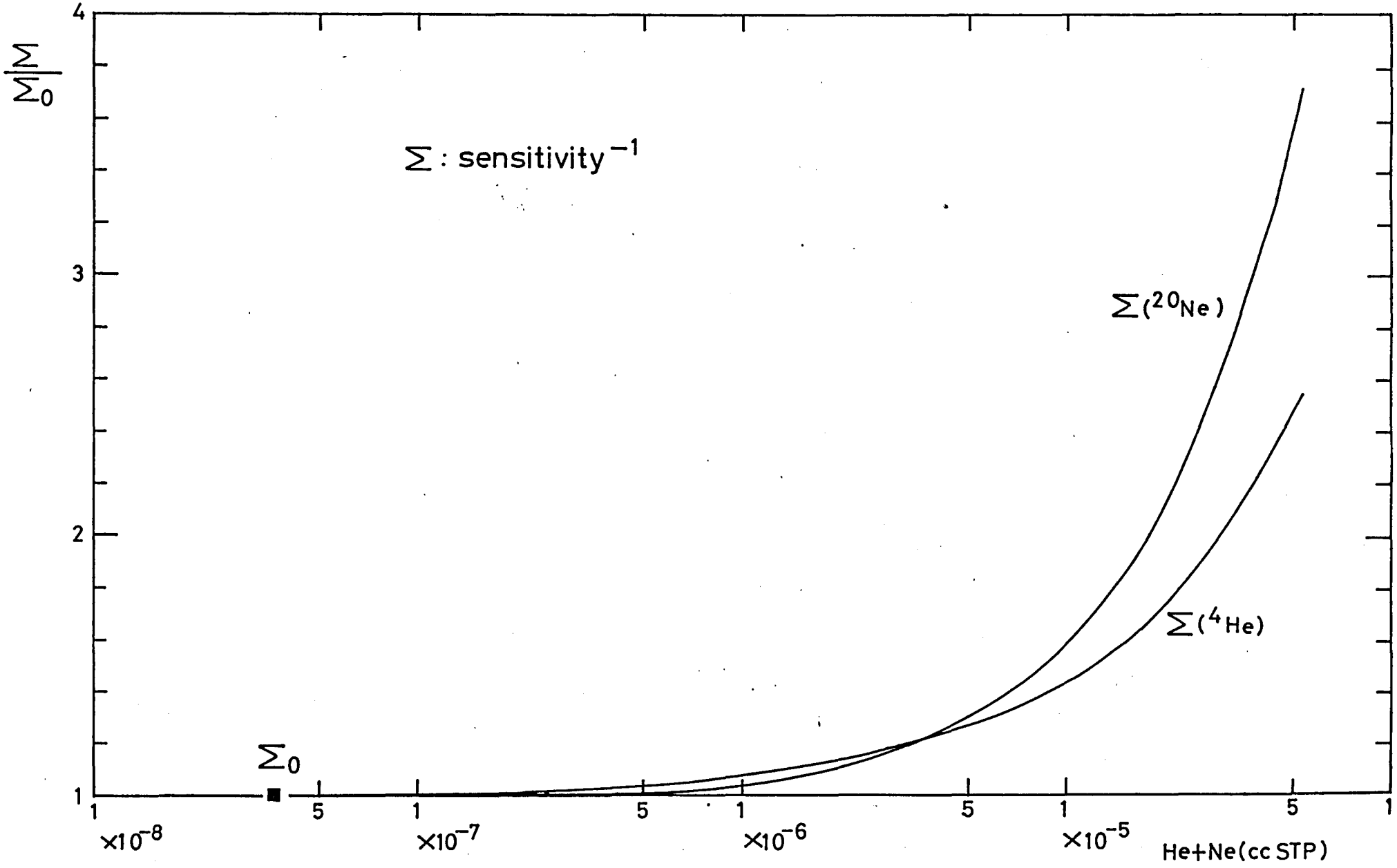
Σ/Σ0
4
3
2
1
Σ : sensitivity⁻¹
Σ(20Ne)
Σ(4He)
Σ0
1
5
1
5
1
5
1
5
1
×10⁻⁸
×10⁻⁷
×10⁻⁶
×10⁻⁵
He+Ne(cc STP)

Fig. Ⅲ-1

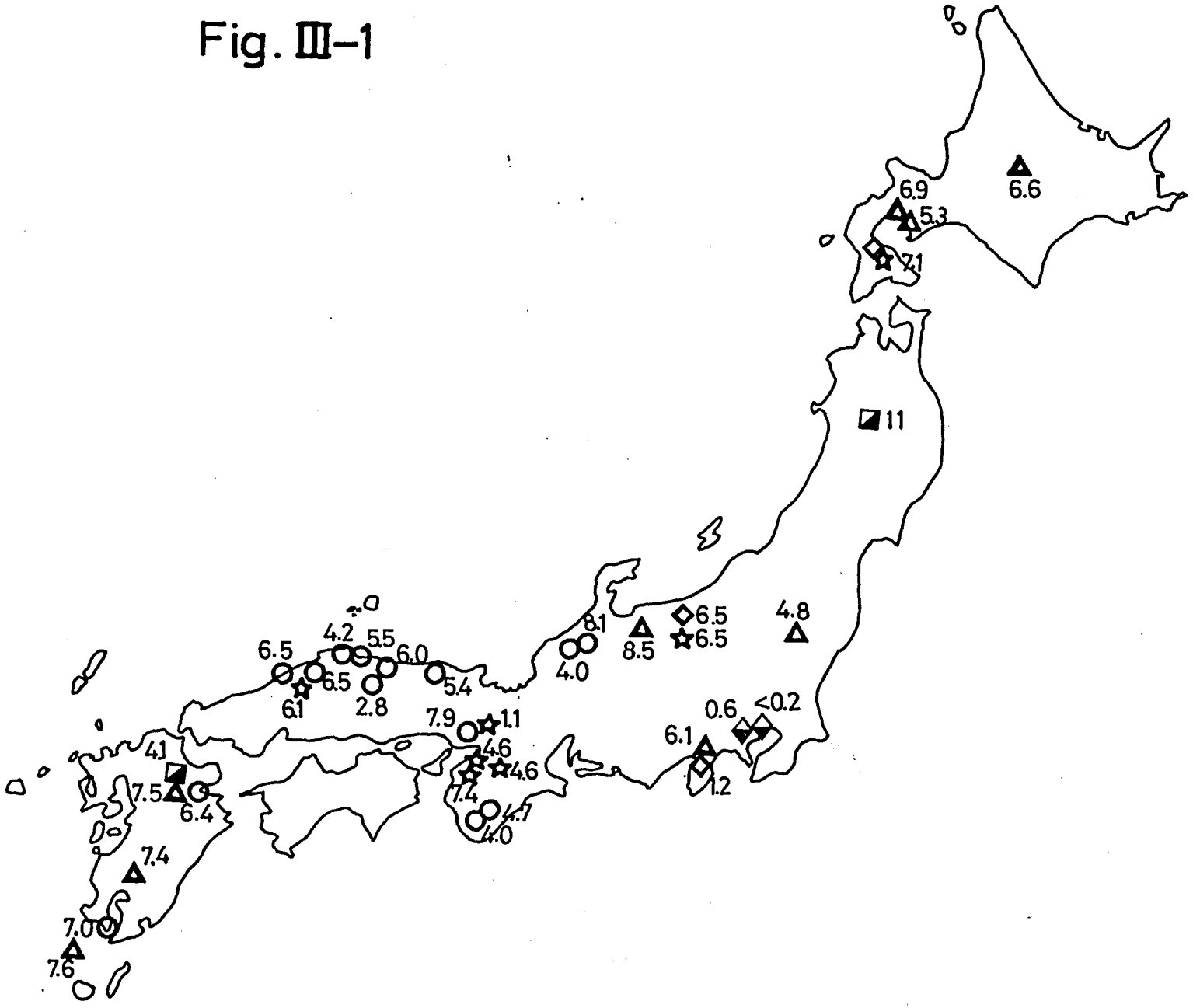
6.9
6.6
5.3
7.1
11
4.8
8.1
6.5
8.5
6.5
4.0
6.5
4.2
5.5
6.0
6.5
5.4
6.1
2.8
7.9
1.1
0.6
<0.2
6.1
4.6
4.6
4.1
7.5
6.4
1.2
7.4
4.1
4.0
7.4
7.0
7.6

Fig. III-2

△ volcanic gas

o hot spring gas

◇ soil gas

⊘ Atlantic Ridge basalt

☆ bubble gas in low temperature water pool

◪ geothermal prospecting well gas

◆ well gas for earthquake prediction

θ continental CO_2 well gas

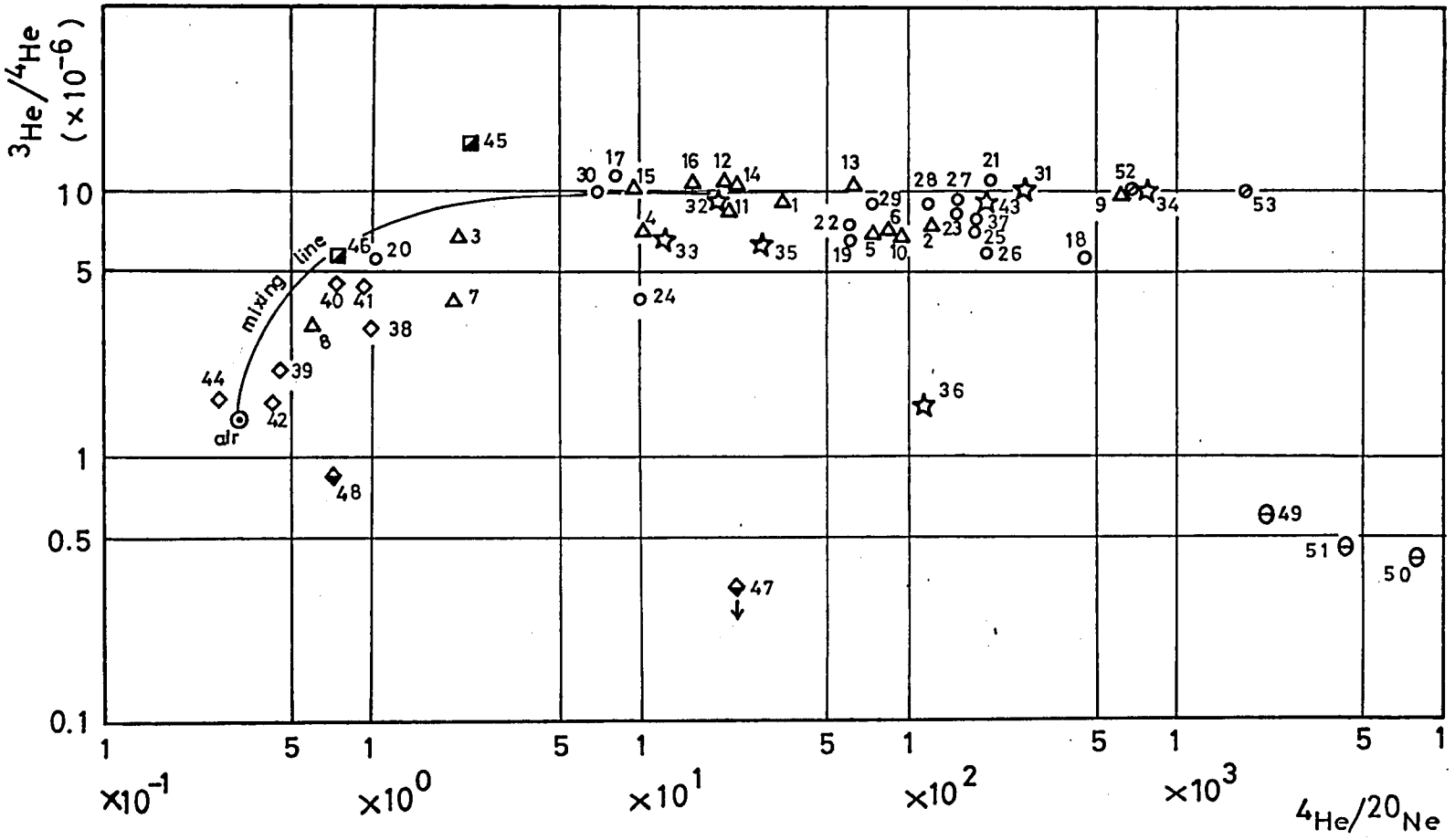

Fig. Ⅲ-3

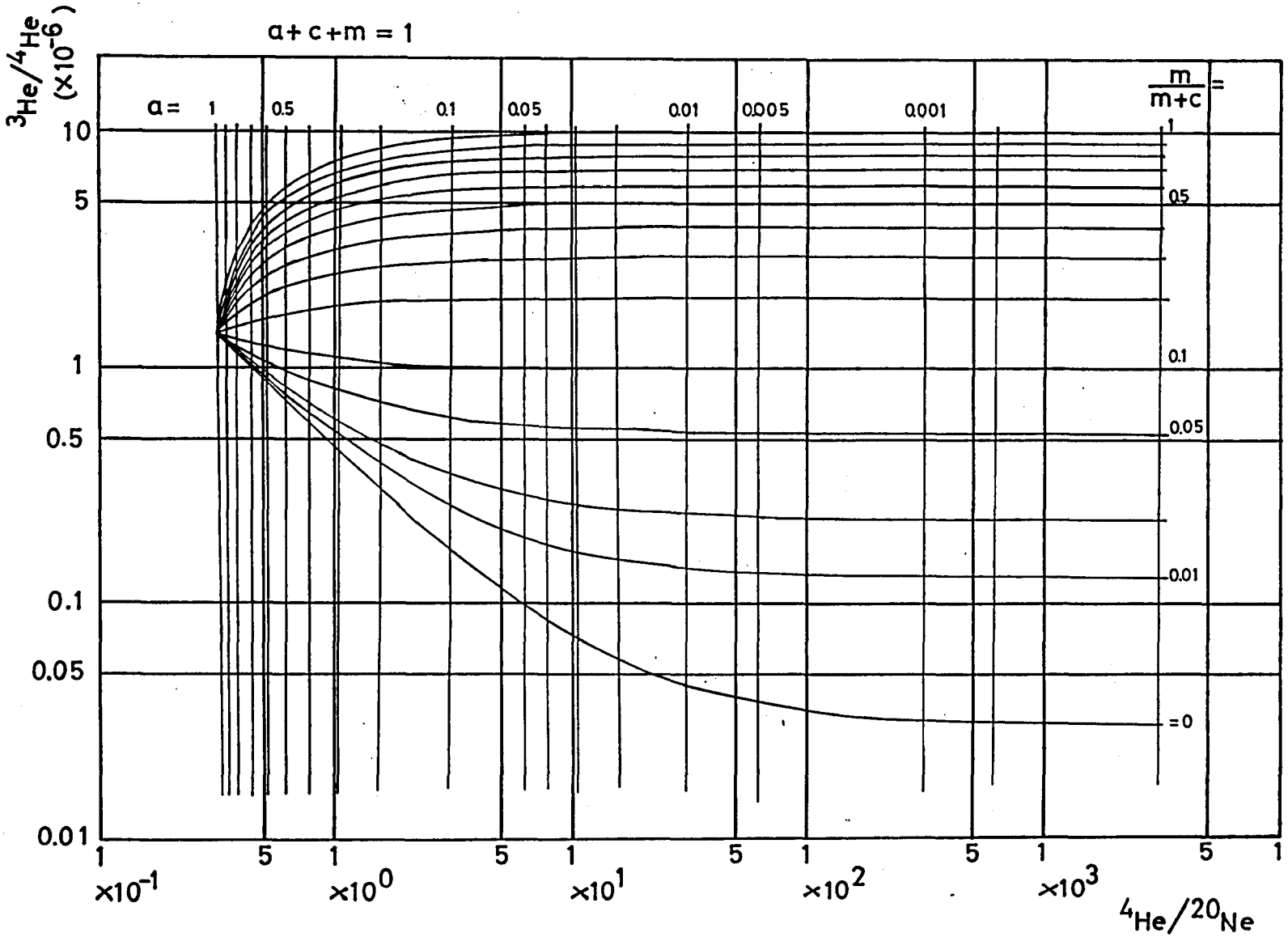
a+c+m = 1
$^3He/^4He$ ($\times 10^{-6}$)
a = 1
0.5
0.1
0.05
0.01
0.005
0.001
$\frac{m}{m+c}$ =
1
0.5
0.1
0.05
0.01
=0
10
5
1
0.5
0.1
0.05
0.01
1
5
1
5
1
5
1
5
1
$\times 10^{-1}$
$\times 10^{0}$
$\times 10^{1}$
$\times 10^{2}$
$\times 10^{3}$
$^4He/^{20}Ne$

Fig. Ⅲ-4

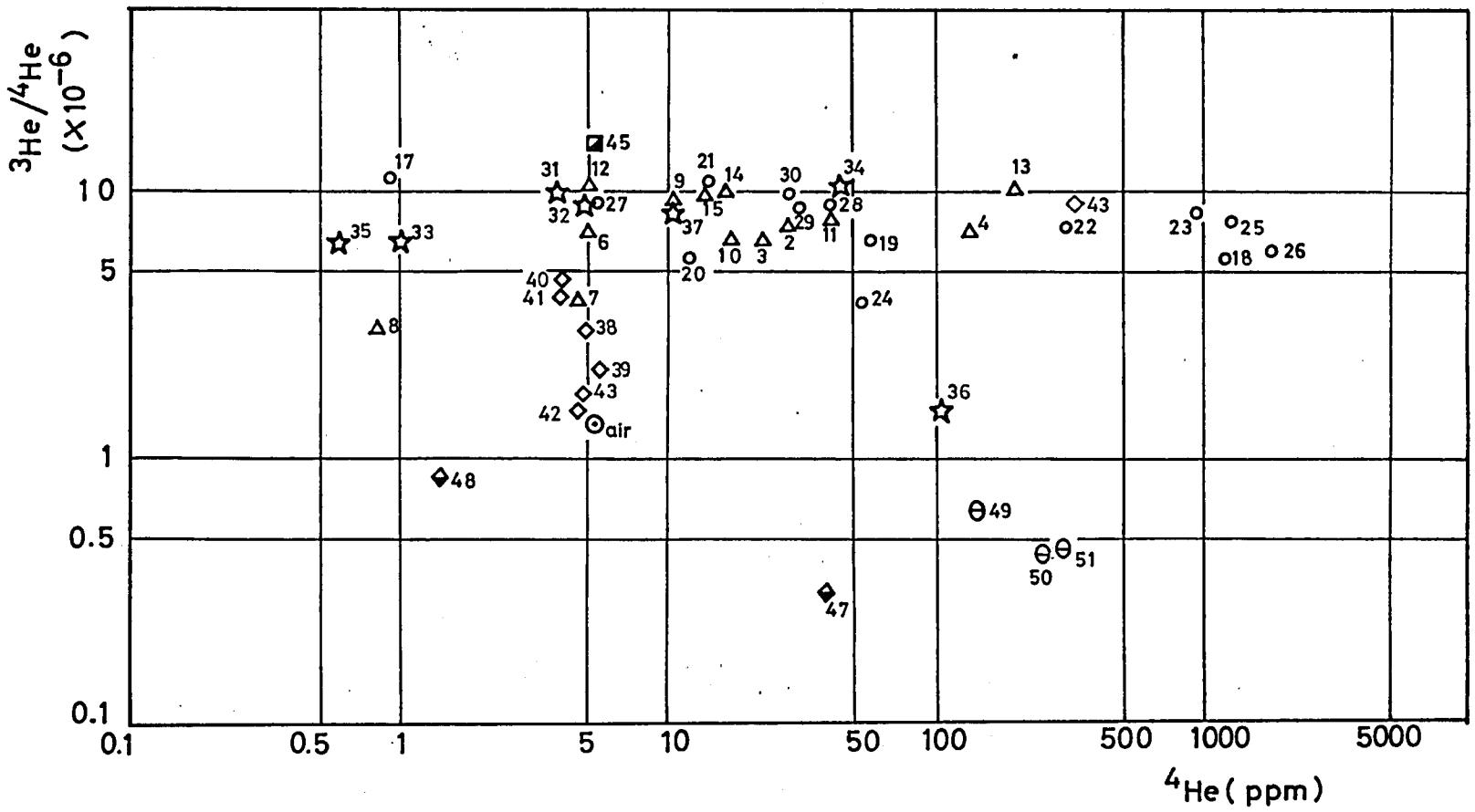
$^3He/^4He$ ($\times 10^{-6}$)
10
5
1
0.5
0.1
0.1
0.5
1
5
10
50
100
500
1000
5000
^4He (ppm)
air

Fig.Ⅲ-5

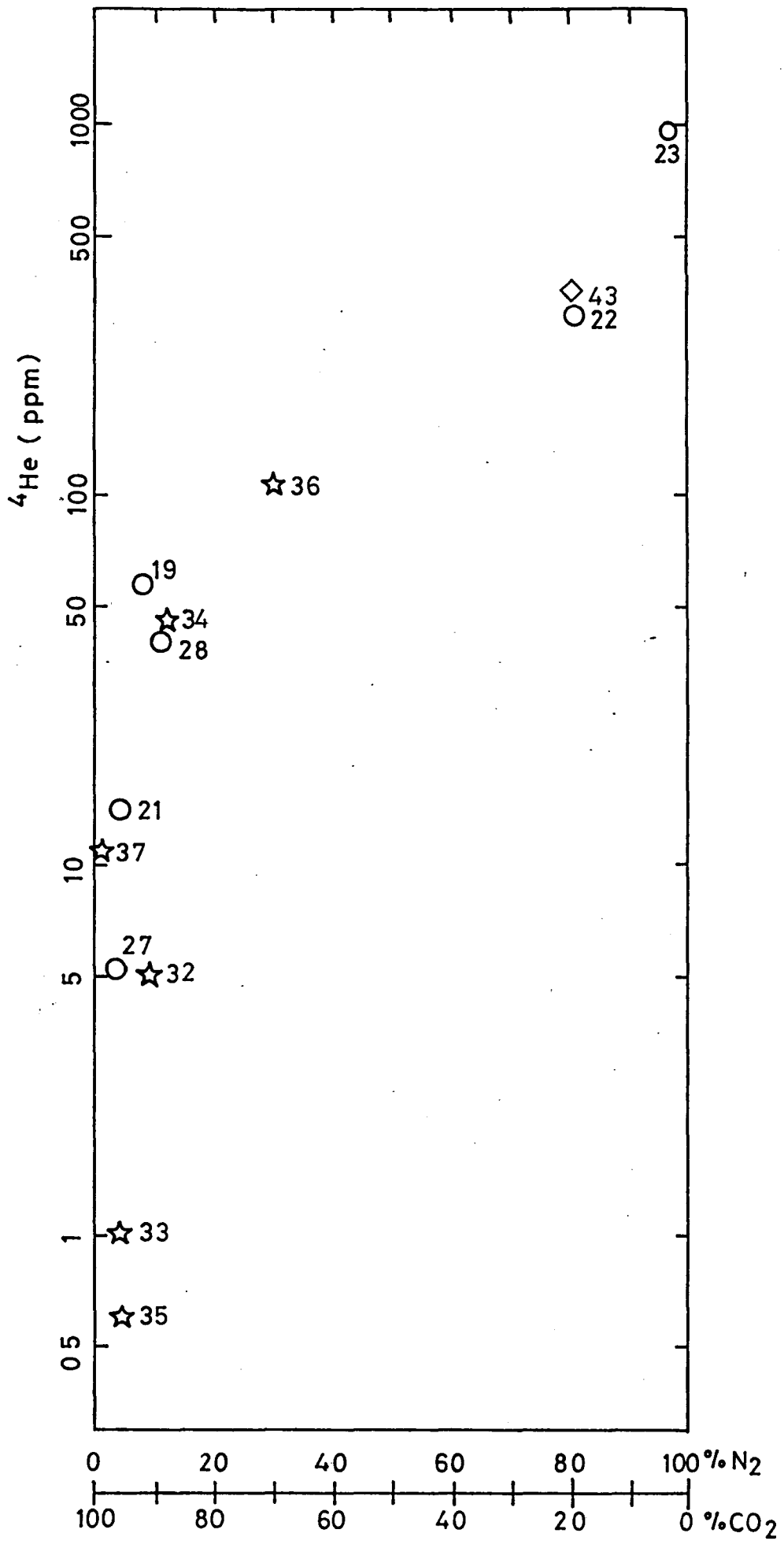
^{4}He (ppm)
1000
500
100
50
10
5
1
0.5
23
43
22
36
19
34
28
21
37
27
32
33
35
0
20
40
60
80
100 %N2
100
80
60
40
20
0 %CO2

Fig. Ⅲ-6

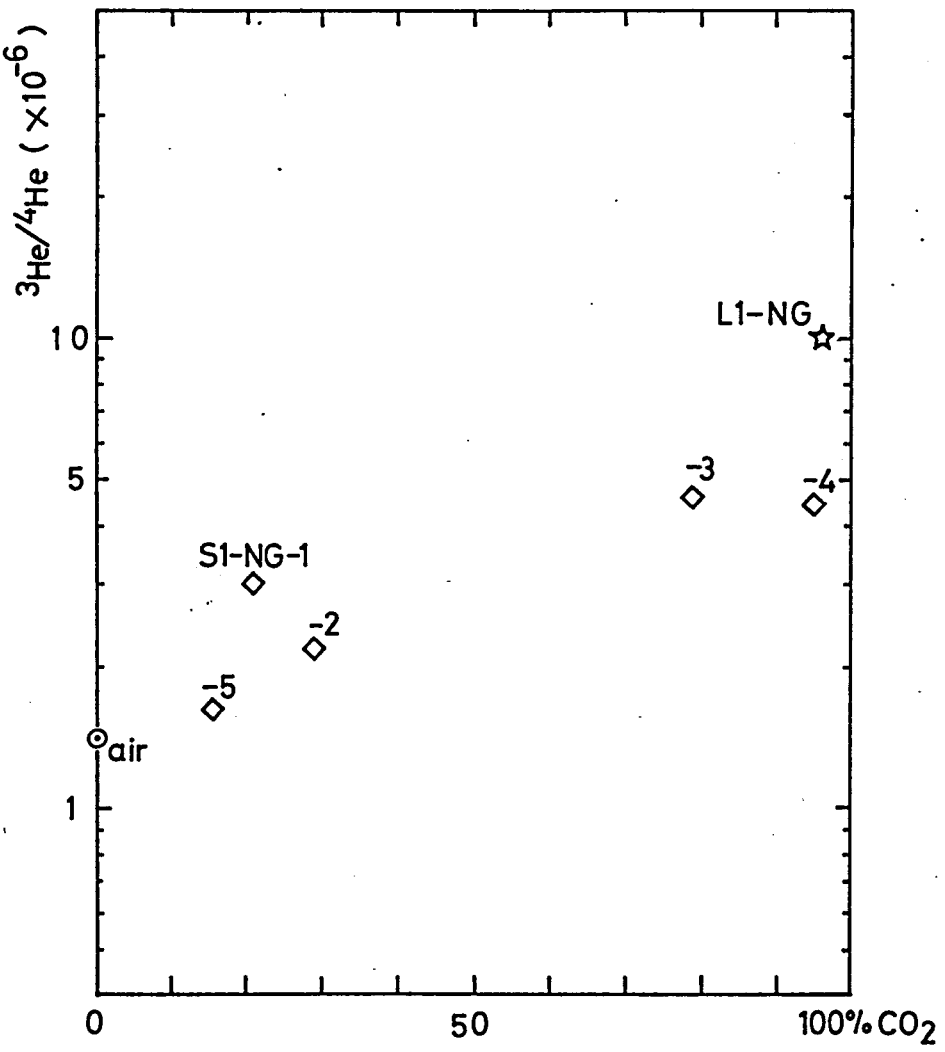

Fig. Ⅲ-7

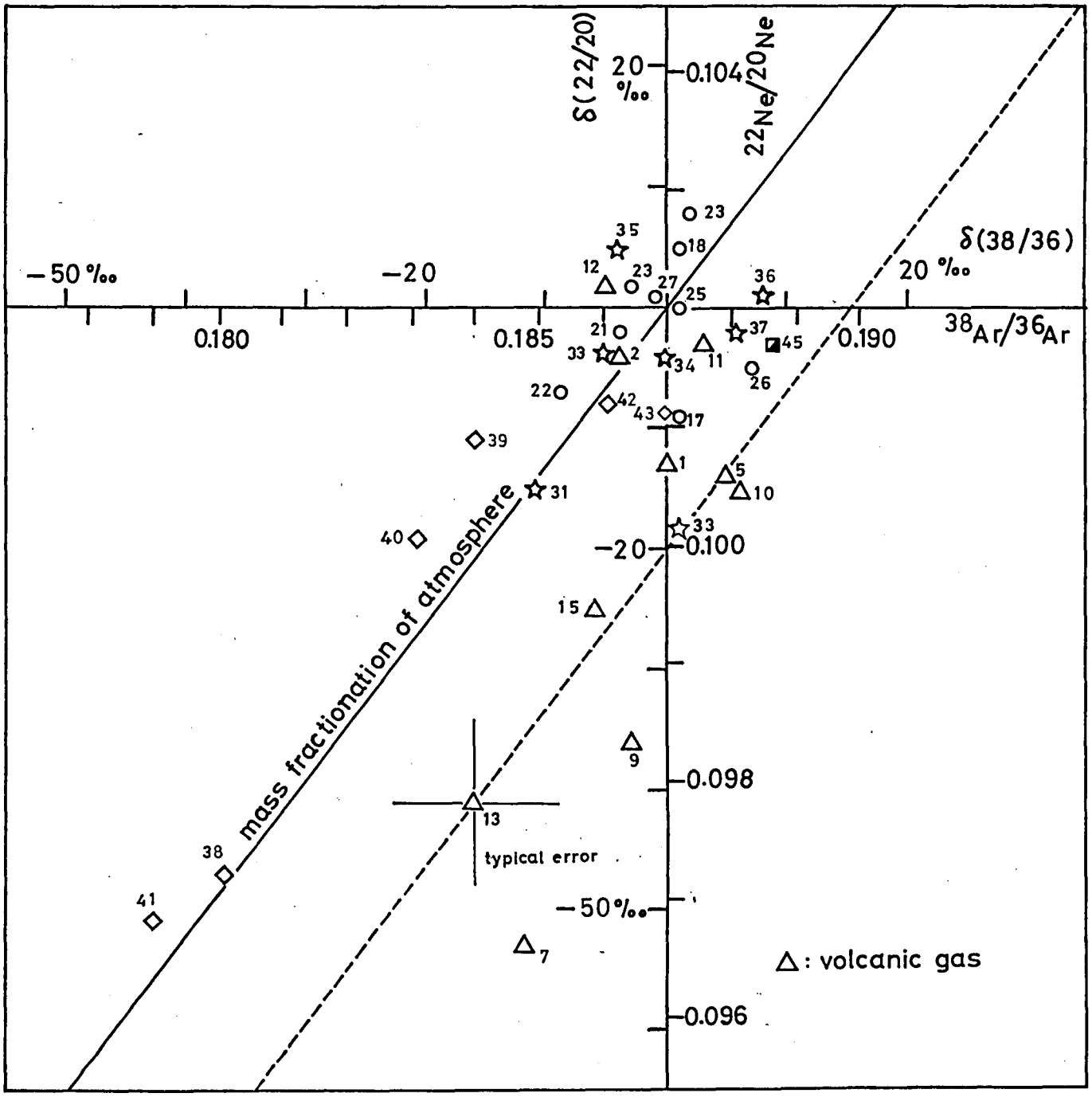
δ(22/20)
20 ‰
0.104
22Ne/20Ne
δ(38/36)
−50 ‰
−20
20 ‰
0.180
0.185
0.190
38Ar/36Ar
0.100
−20
0.098
−50‰
0.096
mass fractionation of atmosphere
typical error
△: volcanic gas

Fig.Ⅲ-8

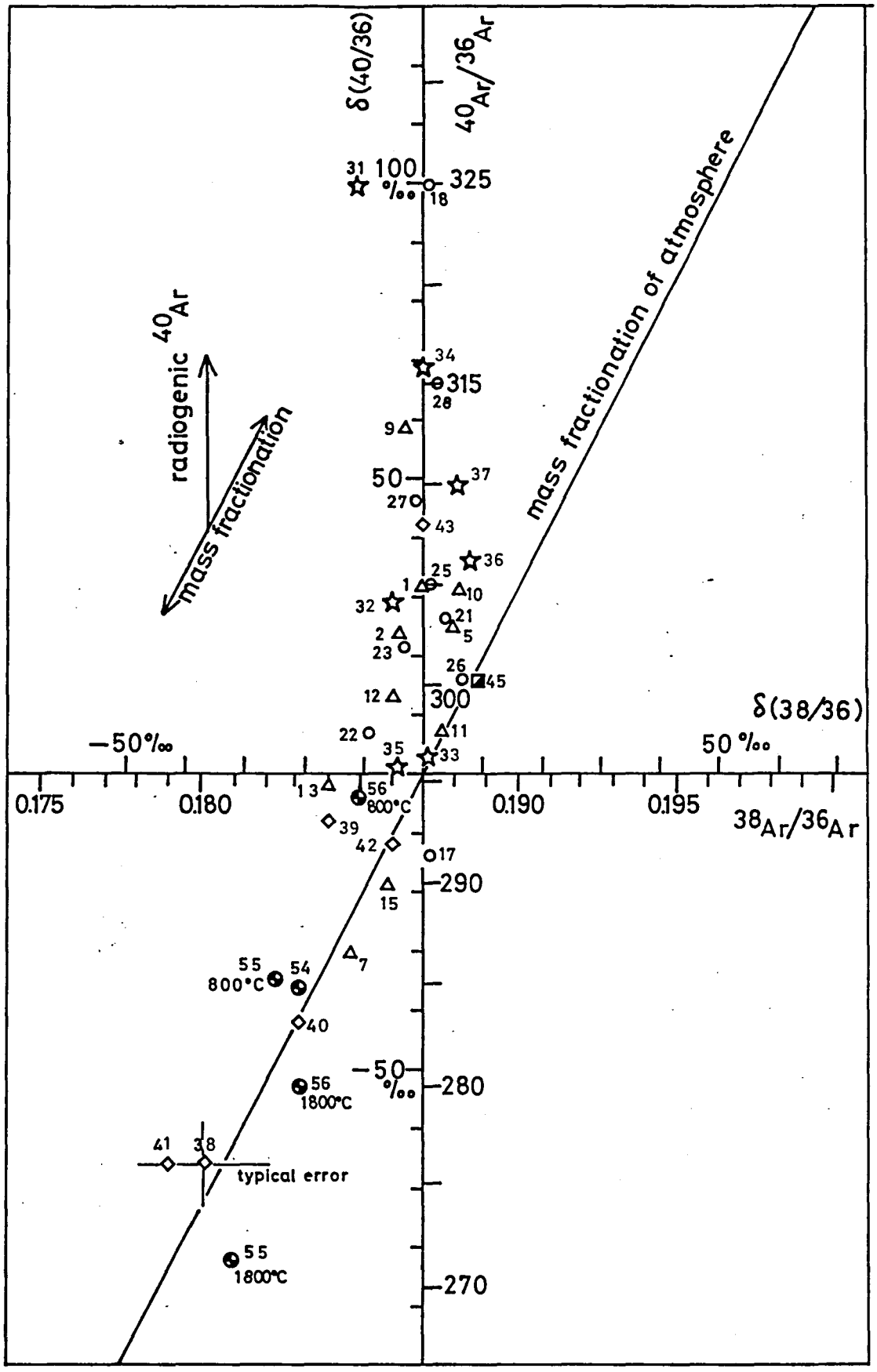
δ(40/36)
40Ar/36Ar
100 ‰
325
315
300
290
280
270
50
-50 ‰
radiogenic 40Ar
mass fractionation
mass fractionation of atmosphere
δ(38/36)
-50‰
50 ‰
0.175
0.180
0.190
0.195
38Ar/36Ar
800°C
1800°C
typical error

Fig. III-9a

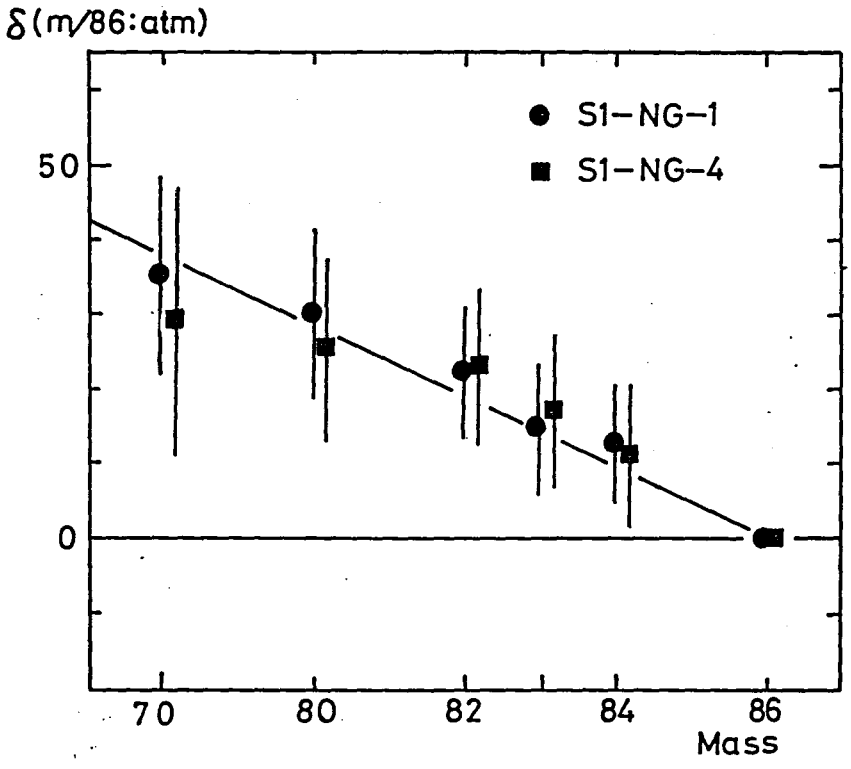

Fig. Ⅲ-9b

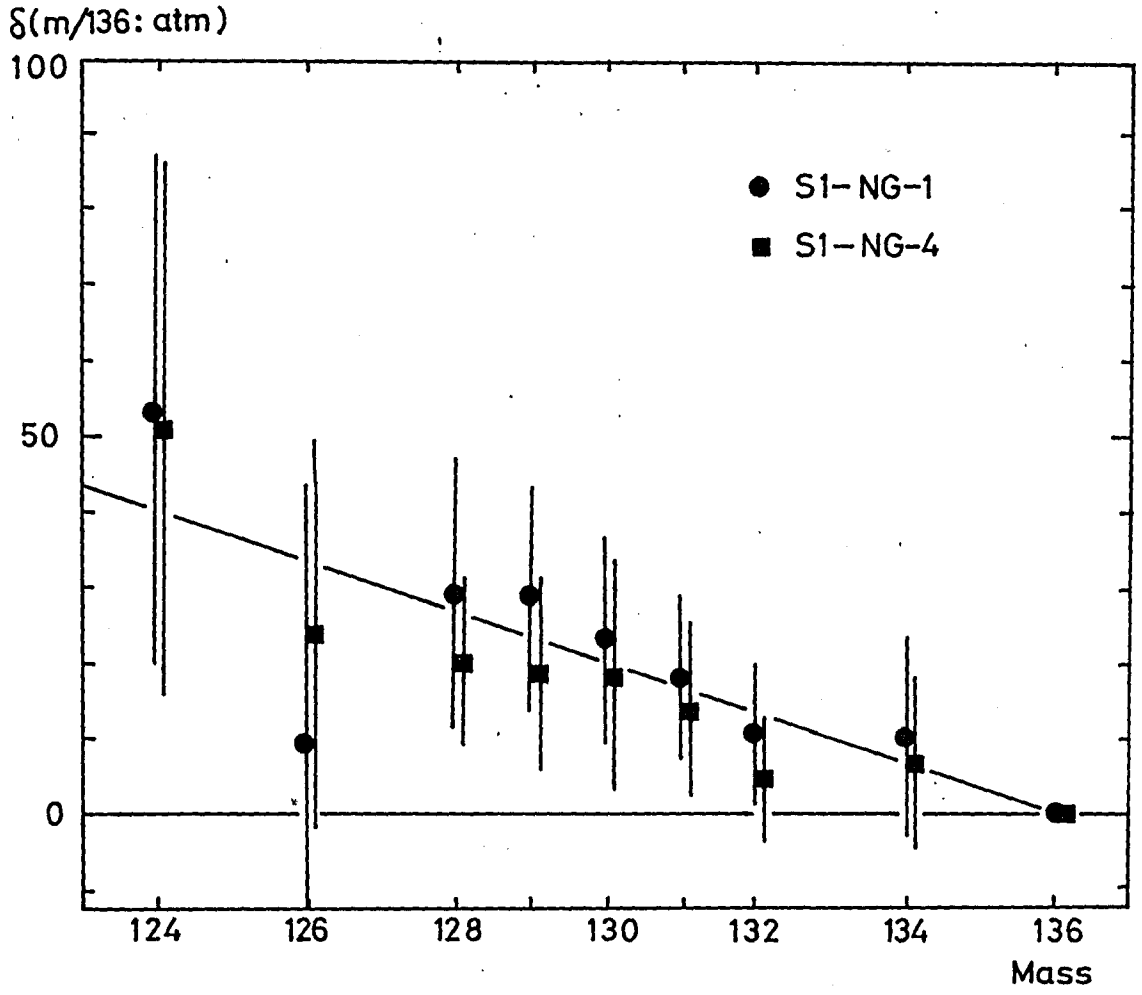

Fig. III-10a

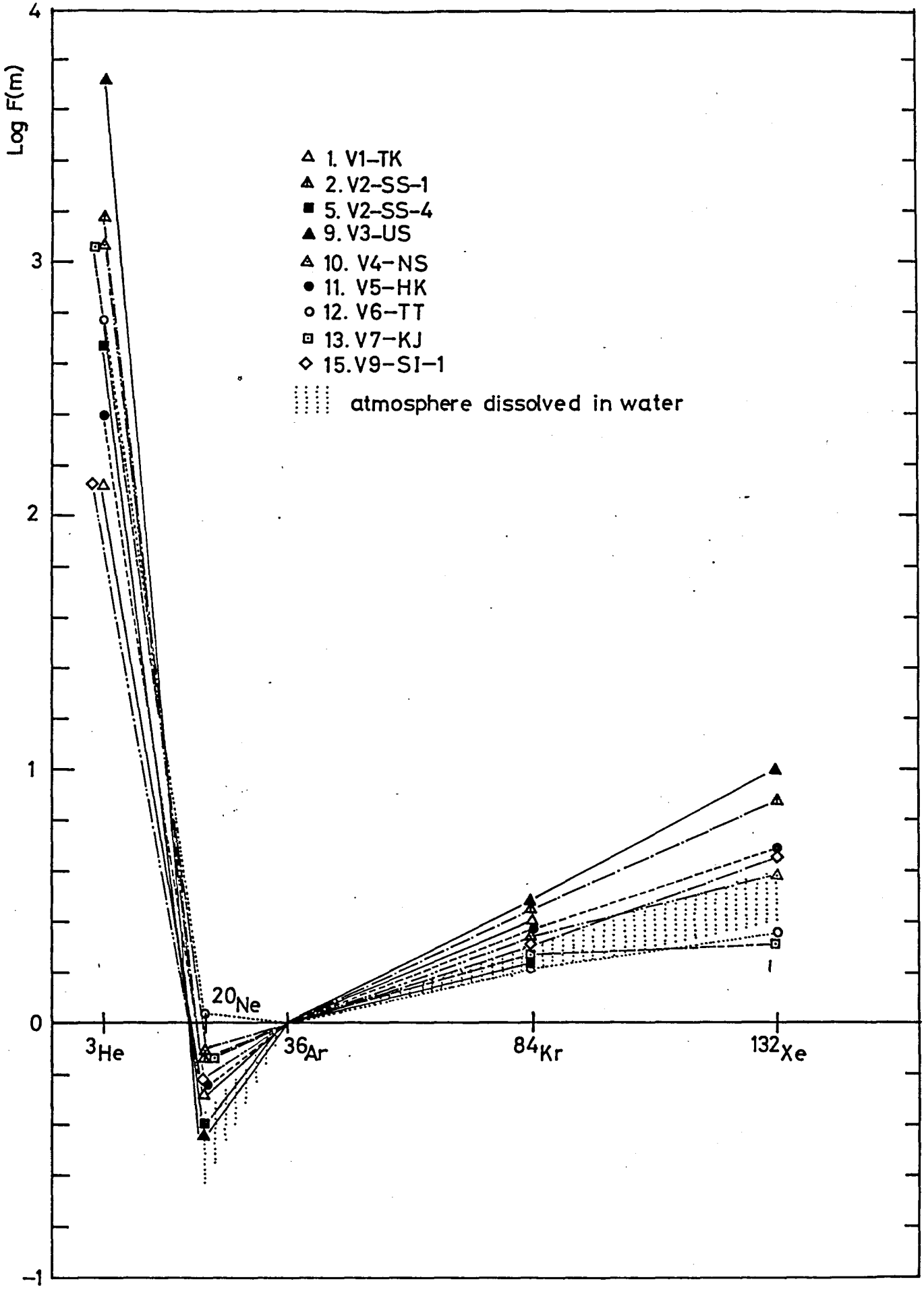
Log F(m)
4
3
2
1
0
-1
1. V1-TK
2. V2-SS-1
5. V2-SS-4
9. V3-US
10. V4-NS
11. V5-HK
12. V6-TT
13. V7-KJ
15. V9-SI-1
atmosphere dissolved in water
20Ne
3He
36Ar
84Kr
132Xe

Fig. Ⅲ-10b

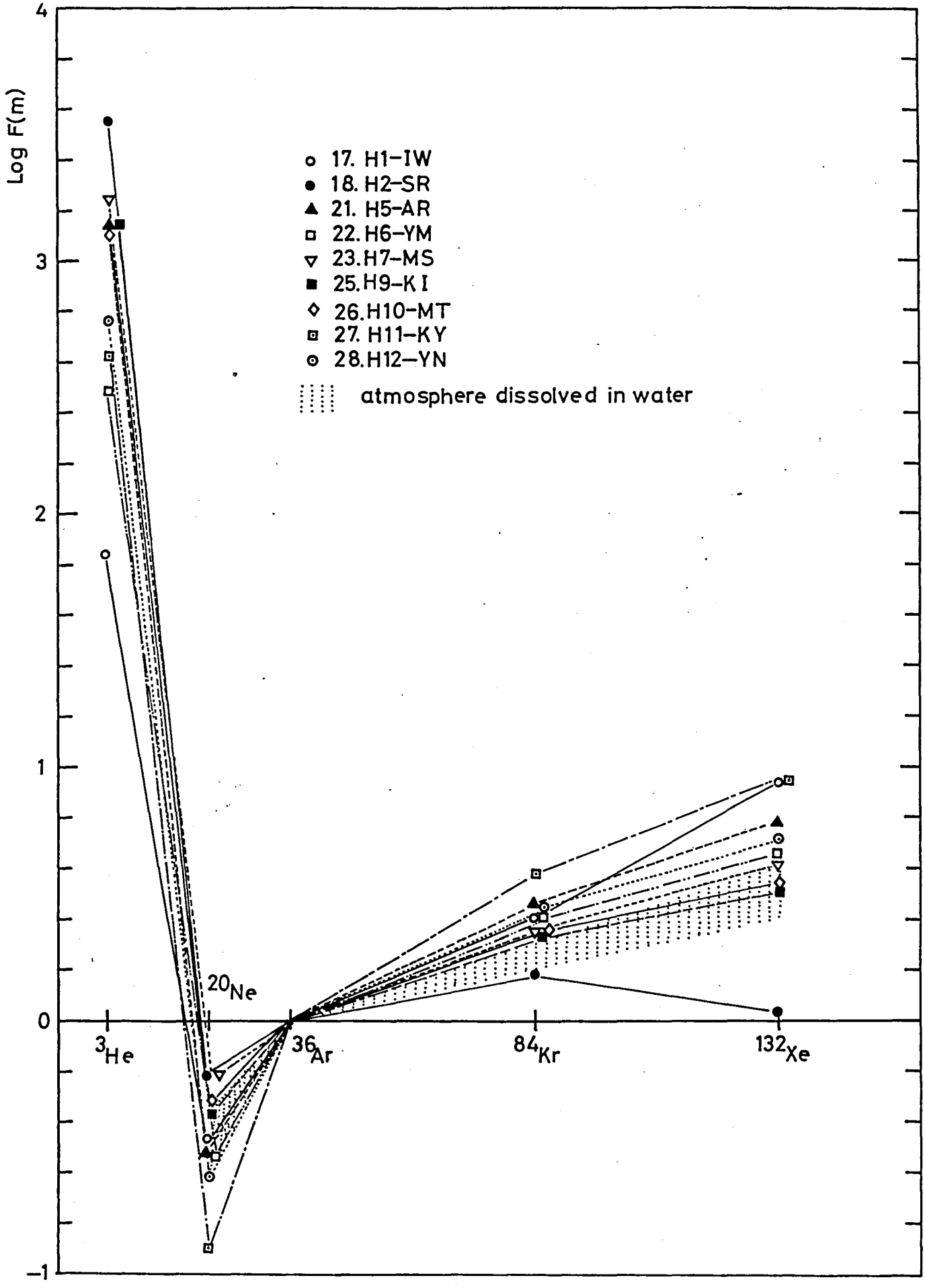
Log F(m)
4
3
2
1
0
−1
17. H1−IW
18. H2−SR
21. H5−AR
22. H6−YM
23. H7−MS
25. H9−KI
26. H10−MT
27. H11−KY
28. H12−YN
atmosphere dissolved in water
^{20}Ne
^{3}He
^{36}Ar
^{84}Kr
^{132}Xe

Fig.Ⅲ-10c

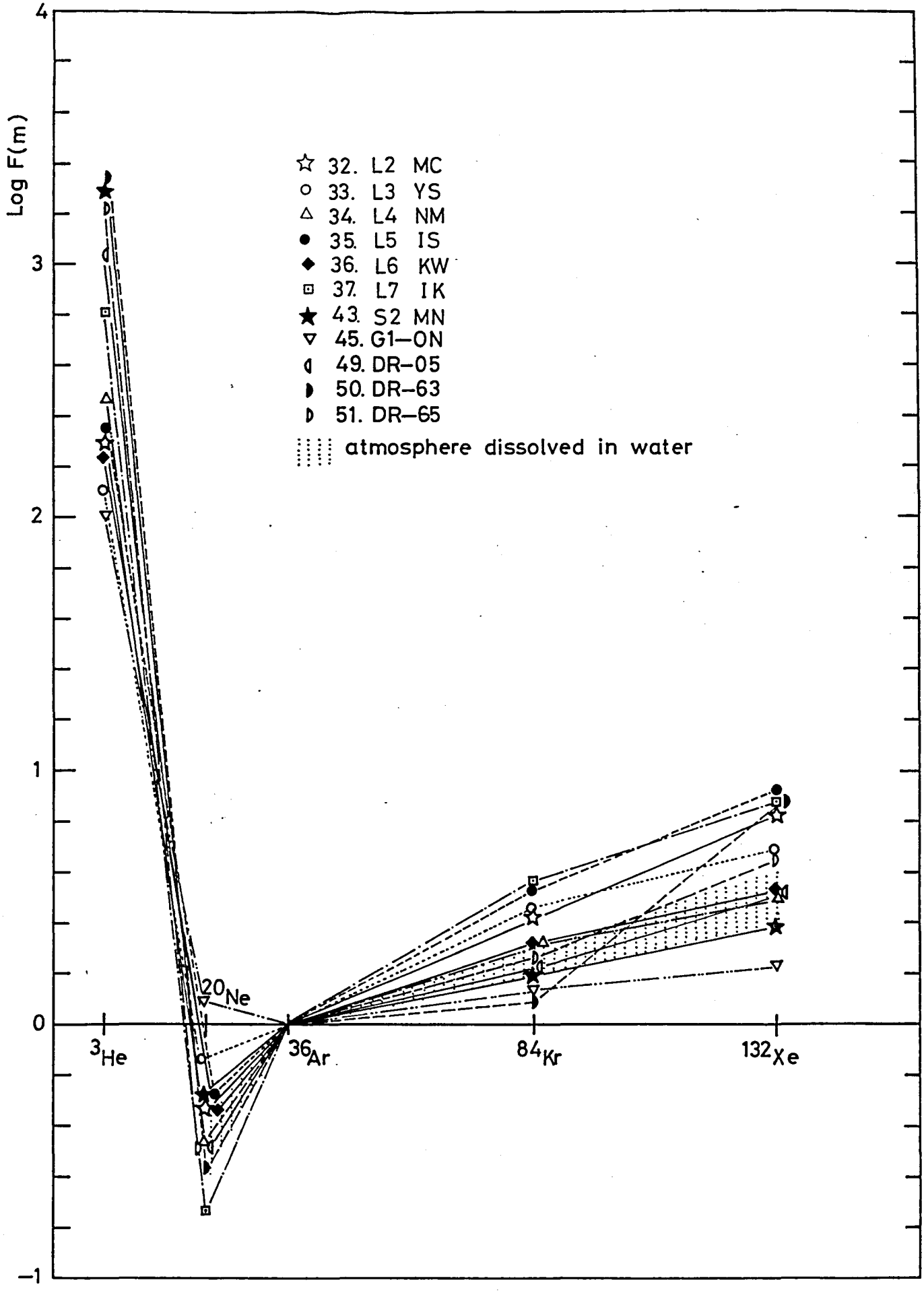
Log F(m)
4
3
2
1
0
−1
32. L2 MC
33. L3 YS
34. L4 NM
35. L5 IS
36. L6 KW
37. L7 IK
43. S2 MN
45. G1−ON
49. DR−05
50. DR−63
51. DR−65
atmosphere dissolved in water
20Ne
3He
36Ar
84Kr
132Xe

Fig.Ⅲ-10d

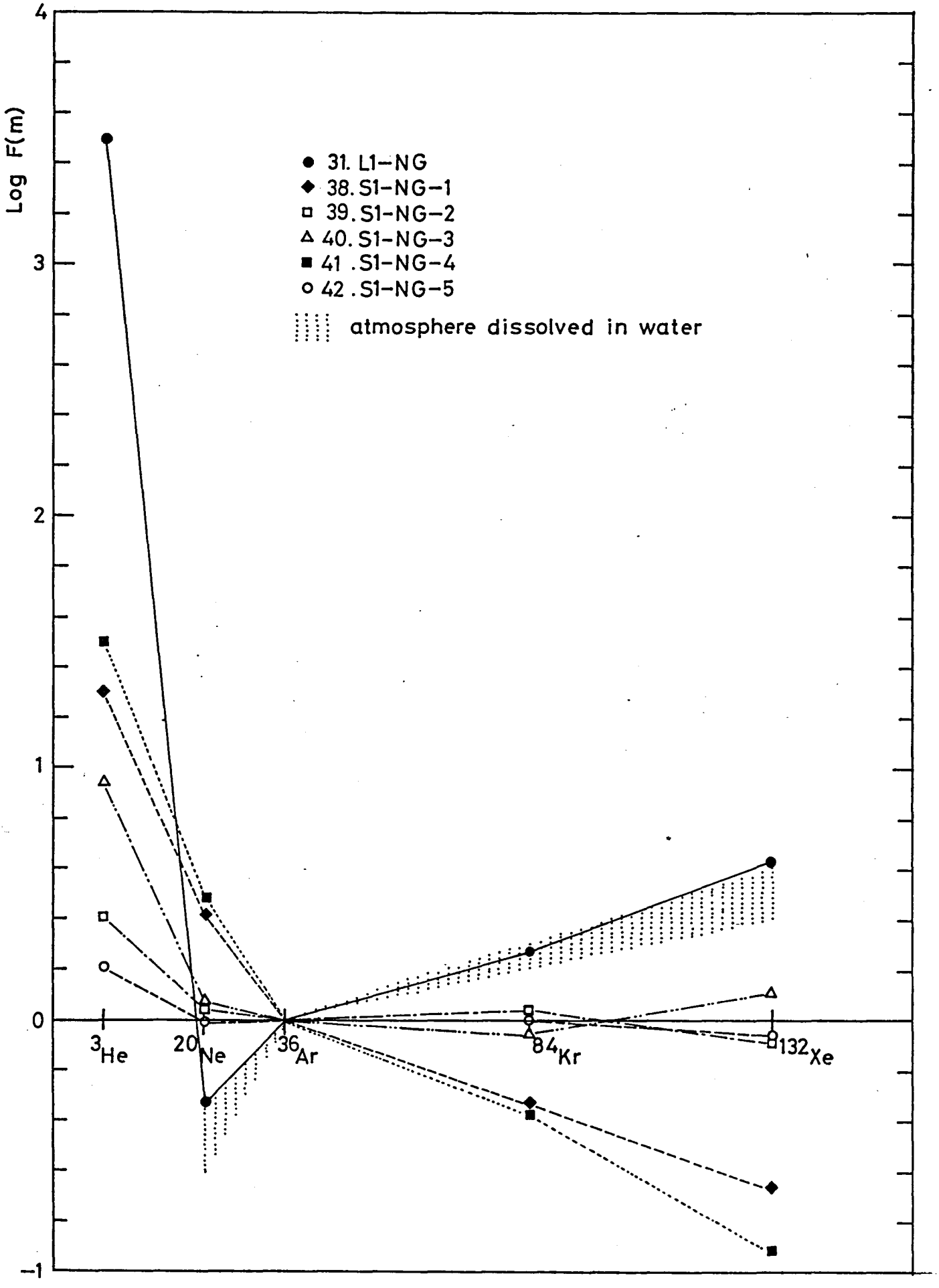
Log F(m)
4
3
2
1
0
−1
● 31. L1−NG
◆ 38. S1−NG−1
□ 39. S1−NG−2
△ 40. S1−NG−3
■ 41 . S1−NG−4
○ 42 . S1−NG−5
atmosphere dissolved in water
3He
20Ne
36Ar
84Kr
132Xe

Fig. IV-1

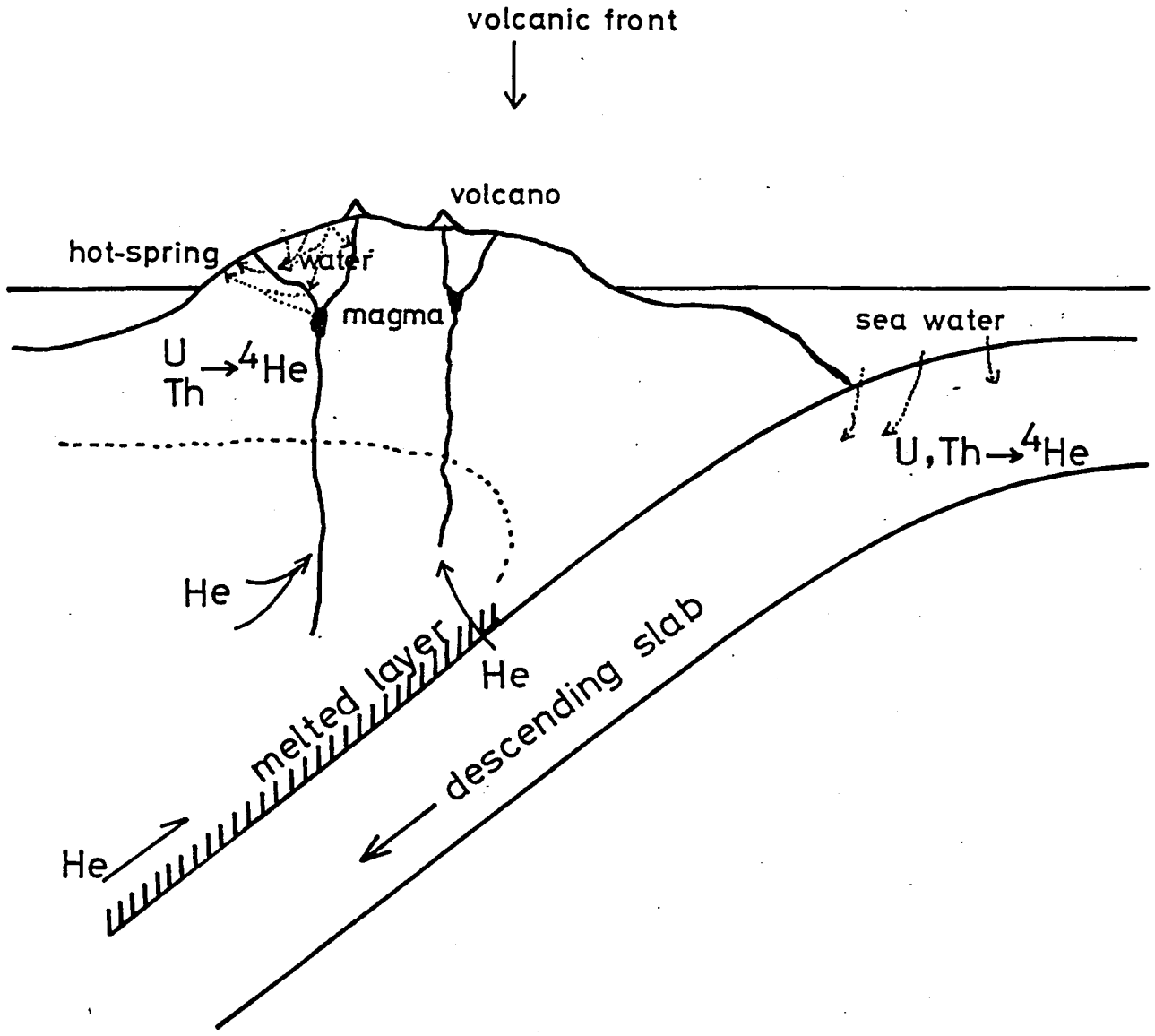
volcanic front
volcano
hot-spring
water
magma
sea water
U
Th
→ 4He
U, Th → 4He
He
He
melted layer
descending slab
He

List of Publications

1) K. Nagao and N. Takaoka, An ion source with electrostatic quadrupole lens pair for rare gas mass spectrometry, Ann. Rept. OULNS(Osaka University, Laboratory of Nuclear Studies), 76-3, 46 (1976).

2) K. Nagao and N. Takaoka, Preliminary studies of concentrations and isotopic compositions of noble gases in the Allende carbonaceous chondrite, Ann. Rept. OULNS, 77-7, 65 (1977).

3) N. Takaoka and K. Nagao, Rare gas studies of Yamato-7301(j), -7304(m) and -7305(k), Memoirs Natl. Inst. Polar Res., special issue 8, 198 (1978).

4) H. Wakita, N. Fujii, S. Matsuo, K. Notsu, K. Nagao and N. Takaoka, "Helium Spots": Caused by a diapiric magma from the upper mantle, Science, 200, 430 (1978).

5) N. Takaoka and K. Nagao, Rare gas studies of Cretaceous deep-sea basalts, "Leg 51-53 Initial Report", DSDP-IPOD (Deep Sea Drilling Project- International Phase of Ocean Drilling), (in press).

6) N. Takaoka and K. Nagao, Isotopic compositions of rare gases in terrestrial and extraterrestrial materials, Ann. Rept. OULNS, 78-2, 56 (1978).

7) K. Nagao and N. Takaoka, Rare gas studies of Antarctic meteorites, Memoirs Natl. Inst. Polar Res., special issue (1979), (in press).

8) K. Nagao, N. Takaoka and O. Matsubayashi, Isotopic anomalies of rare gases in the Nigorikawa geothermal area, Hokkaido, Japan, Earth Planet. Sci. Lett., (in press).

9) N. Takaoka and K. Nagao, Mantle $^{40}Ar/^{36}Ar$ trapped in Cretaceous deep-sea basalts, Nature, 276, 491 (1978).

10) O. Matsubayashi, K. Nagao and N. Takaoka, Magmatic isotopic anomaly of He found in various natural gases along the Japanese Islands, Bull. Volcanol. Soc. Japan, (in Japanese) (in press).